Sustainable Astronomy: A comparative Life Cycle Assessment of Off-grid Hybrid Energy Systems to supply large Telescopes

Isabelle Viole (isabelvi@uio.no)
Department of Technology Systems, University of Oslo https://orcid.org/0000-0002-5020-2394
Li Shen
Copernicus Institute of Sustainable Development, Utrecht University https://orcid.org/0000-0001-9378-7372
Luis Ramirez Camargo
Copernicus Institute of Sustainable Development, Utrecht University https://orcid.org/0000-0002-1554-206X
Marianne Zeyringer
Department of Technology Systems, University of Oslo
Sabrina Sartori
Department of Technology Systems, University of Oslo https://orcid.org/0000-0002-9952-6488

Research Article

Keywords: Life cycle assessment, Off-grid energy system, Hybrid energy storage system, Astronomical observatories, Carbon intensity, Sustainable research facilities

Posted Date: August 23rd, 2023

DOI: https://doi.org/10.21203/rs.3.rs-3281965/v1

Abstract

Purpose

Supplying off-grid facilities such as astronomical observatories with renewable energy-based systems (RES) instead of diesel generators can considerably reduce their environmental impact. However, RES require oversized capacities to counter intermittency and comply with reliability requirements, hence shifting the environmental impact from operation to construction phase. We assess whether 100% RES scenarios are favorable from an environmental point of view, and discuss the trade-offs in systems with backup fossil generators versus 100% renewable ones.

Methods

In this comparative life cycle assessment (LCA), we study various RES supply systems to power a new telescope in the Atacama desert, Chile. We compare six setups, including 100% RES scenarios, namely photovoltaics (PV) with batteries and hydrogen energy storage; high-renewable scenarios, with fossil fuel power generation next to RES and storage; and a system combining PV with diesel generation. We base system sizing on a techno-economical optimization for the start of operation in 2030. Foreground data stem from recent life cycle inventories of RES components and 2030 electricity mix assumptions of production places. We assess environmental impact in the categories climate change, mineral resource depletion and water use.

Results and discussion

We find that 100% RES and high-renewable scenarios result in emissions of 0.077-0.115kg CO_2e/kWh supplied, compared to 0.917kg CO_2e/kWh in the reference case with solely diesel generation. 100% RES scenarios have a lower CO_2e impact than high-renewable scenarios. However, the latter lower the mineral resource depletion and water use by about 27% compared to 100% RES scenarios. Applying hybrid energy storage systems increases the water use impact, while reducing the mineral resource depletion.

Conclusions

None of the six energy systems we compared was clearly the best in all environmental impacts considered. Trade-offs must be taken when choosing an energy system to supply the prospective off-grid telescope in Chile. We find high-renewable systems with some fossil generation as the better option regarding power reliability, mineral resource depletion and water use, while inducing slightly higher greenhouse gas emissions than the 100% RES scenarios.

As remote research facilities and off-grid settlements today are mainly supplied by fossil fuels, we expect to motivate more multifaceted decisions for implementing larger shares of RES for these areas. To advance the LCA community in the field of energy systems, we should strive to incorporate temporal and regional realities into our life cycle inventories. To ease the path for upcoming studies, we publish this work's inventories as detailed activity level datasets.

1. Introduction

Scientific projects need to considerably lower their environmental impacts to contribute to a society that can flourish without surpassing planetary boundaries. In the field of ground-based astronomical observatories the median carbon intensity per paper published reaches 24t CO_2 equivalents (CO_2e), including both the construction and operation of the observatory (Knödlseder et al. 2022). In comparison, the carbon footprint per capita in 2019 amounted to 4.8t CO_2e in Chile and to 6.8t CO_2e in the European Union (EU) (World Bank n.d.).

The operational emissions of remote and off-grid telescopes primarily stem from their reliance on fossil fuel generators to meet their energy needs. This demand of mainly electrical energy is needed to power the dish motors, and supply the cryogenic cooling for the instruments. In recent years, first measures have been taken to address this issue in astronomy and some observatories integrated photovoltaic arrays (PV) into their energy systems, which lowers their direct greenhouse gas (GHG) emissions during sunny hours (Rodríguez 2022). However, off-grid energy systems worldwide are overly reliant on fossil fuels for their power generation, as seen in remote settlements on Svalbard in the Arctic, in deserts in the Middle East or in rural locations in Sub-Saharan Africa (Ringkjøb et al. 2020; Ghenai et al. 2020; Olabode et al. 2021). This reliance must change to mitigate global warming.

The Atacama Large Aperture Submillimeter Telescope (AtLAST) project, which is designing a new transformational telescope to be built on the Chajnantor plateau in the Atacama Desert in Chile, is pioneering a shift towards sustainable practices. It is the first astronomical observatory project that includes plans for an off-grid, completely renewable energy system right from its design phase (Klaassen et al. 2020; Ramasawmy et al. 2022). The results of this project will inform future efforts in other remote locations.

In our previous techno-economical analysis of AtLAST's energy system, we conducted a comparison between a business-as-usual scenario with conventional diesel generation and various combinations of PV, hybrid energy storage systems (HESS), and diesel generators over a 25-year lifetime (Viole et al. 2023b). The AtLAST telescope, which will have a 50-meter diameter primary mirror and will operate at both day and night, has an expected daily energy demand of $22MWh_e$, which exhibits relative stability on an intraday basis but varies seasonally due to the addition or removal of instruments. Considering cost estimates for the projected construction year of 2030, the system with the minimal costs identified in Viole et al. (2023b) comprised a $4.8MW_p$ PV park, 14.2 MWh of Lithium-ion batteries, a hydrogen system including a $0.34MW_e$ electrolyzer, a $0.39MW_e$ fuel cell and a 160 kg hydrogen storage tank. Diesel generators were included as backup to meet approximately 5% of the energy demand. This system achieved a 95% reduction in direct GHG emissions, measured in CO_2e, compared to relying on diesel generators only. To achieve 0% direct CO_2e emissions, the PV park would need to be expanded by 42% to fuel the larger storage needs for green hydrogen production and battery charging.

1.1 Life cycle assessment (LCA) for renewable energy systems

Building the larger PV park with zero direct emissions increases the environmental impact of the production phase of renewable energy-based systems (RES). A techno-economical energy system optimization that solely takes direct GHG emissions from the operation phase into account paints a slanted picture of the CO_2e emissions, giving the appearance that 100% RES would always be favorable from an environmental point of view. To counter this, we can add or include a LCA onto the energy system optimization. Previous applications of *ex-post* LCAs on national energy system models incorporating RES have generally shown that higher shares of RES reduce climate change impacts but lead to increased mineral depletion (Hertwich et al. 2015; Berrill et al. 2016). A literature review on electricity generation LCAs found that most studies identify RES to have lower life cycle GHG emissions compared to their fossil counterparts (Barros et al. 2020). Most of the reviewed studies relied on the ecoinvent database for their life cycle inventories (LCI), that is the underlying datasets used to receive the final environmental impact calculation. These ecoinvent LCIs have a global scope, which can distort results for specific locations, and are not regularly updated. For instance, the datasets for PV cell production in ecoinvent 3.7.1 (such as “Photovoltaic cell, single-Si wafer {RoW}| production | Cut-off, U”) are based on data that are two decades old. Tannous et al. (2019) found that environmental impacts of PV production have declined by 21–50% compared to ecoinvent 3.4 datasets from 2005, which they associate with technological advancements in electricity consumption and manufacturing processes. Therefore, it is crucial for the research field to strive for better data quality by utilizing local characteristics and more up-to-date datasets.

Local characteristics are particularly relevant in stand-alone or off-grid systems, such as the one discussed for AtLAST. These small- to mid-scale energy systems are influenced by the weather conditions of one specific zone, which amplifies the intermittent nature of RES generation. Additionally, they have limited or no connection to a centralized grid that could help balance the systems. LCAs on remote energy systems have been conducted e.g. in Marsabit, Kenya; Alaska, USA; and Ginostra, Italy (Bilich et al. 2017; McCallum et al. 2021; Gandiglio et al. 2022). These studies employed different approaches, ranging from cradle-to-gate analyses to including end-of-life scenarios. They compared predefined RES, such as hydropower; PV paired with batteries; or PV, batteries and hydrogen storage, with the previously used diesel generators in the respective areas. The findings consistently showed that the implementation of RES systems reduced the GHG impact by 88–99%. In Gandiglio et al. (2022)’s study, the renewable scenario based on PV and lithium-ion (Li-ion) batteries decreased CO_2e emissions by -88.6% over the 25 years lifetime, while mineral and metal resources increased by + 80%, and the water use by + 61%. McCallum et al. (2021) studied the deployment of hydropower paired with Li-ion batteries in remote Alaska, and suggested deployments of 10 or 20 years to reduce the impacts in water and metal depletion, which are linked with the metal used in the system. Bilich et al. (2017) found their PV and battery setup to significantly decrease the climate change environmental impact compared to home diesel gensets, however did not consider mineral resource depletion or water use. They noted that setting up such a PV and battery system for a rural Kenyan community could result in load-shedding issues and suggested mitigating this by installing a backup diesel generator.

Off-grid energy systems face unique challenges, as they cannot rely on a national electricity grid to balance fluctuations in power generation from intermittent RES. Optimizing off-grid energy systems with high shares of RES presents two main issues. Firstly, it can result in more frequent load shedding, which is not feasible for operating a telescope or other critical applications. Secondly, it often requires oversizing components in combination with batteries to buffer out the variability in supply, including unfavorable weather periods. As a solution, fossil fuel-based generators are commonly added as a backup alongside PV and batteries, as they offer lower levelized costs of electricity (LCOE) by avoiding the high capital costs of surplus RES capacities (Odou et al. 2020; Come Zebra et al. 2021). In a review of off-grid energy systems in developing countries, Come Zebra et al. (2021) found that energy systems combining RES and diesel generators are financially more attractive compared to 100% renewable systems.

To enhance the reliability of off-grid RES-based systems and minimize the need for excessive built capacity, another option is the integration of HESS. These systems combine multiple energy storage technologies, such as batteries for short- to medium-term energy storage, with a hydrogen system for medium- to long-term energy storage (Bocklisch 2015). Many off-grid energy system optimizations propose the usage of HESS and some real scale tests have been conducted already, such as by Endo et al. (2019) and at the Sir Samuel Griffith Centre (HyResource 2020), and are also under consideration for the telescope project AtLAST. To our knowledge, no LCA comparison between HESS to systems relying on one energy storage has been conducted thus far in either grid-connected or off-grid setups.

We identify a number of research gaps in literature: First, most studies on specific energy system case studies use global LCIs, while the quality of the LCA could be improved by using temporal- and site-specific datasets. This especially is relevant concerning the electricity mixes of the production locations of RES components, as e.g. the carbon intensity of this production has a major influence on the life cycle environmental impact of the systems considered. Second, to our knowledge, there is no LCA on off-grid energy systems that includes up-to-date LCIs that are in line with recent technological developments. Further, LCAs on islanded or off-grid energy systems have so far mainly been carried out comparing one or two RES options to a business as usual fossil scenario. A broad comparison of different renewable systems, such as those with HESS to those only using batteries, or a comparison of 100% RES scenarios to high-renewable scenarios with mostly RES and some fossil generation backup is lacking and can paint a more faceted picture of the environmental impacts.

1.2 Designing a site- and temporal-specific LCA study for a telescope in the Atacama

In this work we contribute to close these gaps by: 1. Conducting the first LCA on off-grid energy systems with recent LCIs and recent projections of power mixes in the production locations, putting an emphasis on site-and temporal-specific inputs. 2. Considering five different scenarios of implementing RES into the energy system for AtLAST, 100% RES to high-renewable systems, and batteries with HESS. This allows us to identify trade-offs between the use of different components.

Specifically, the objective of this work is to find the environmental impacts of the off-grid renewable energy systems that can supply the $22MWh_e$/day and $7.7GWh_e$/year energy needs of AtLAST. We conduct a comparative life cycle assessment (LCA) to evaluate three impact categories: 1. Depletion of mineral resources, 2. Water use, and 3. Climate change impact both from direct and indirect emissions. This study examines the cradle-to-gate environmental impacts of different energy system configurations for the telescope in question, combining an *ex-post* LCA with the findings from the highRES-AtLAST energy system optimization model, developed by Valenzuela Venegas (2022), see methodology flowchart in Fig. 1. We adopt a specific temporal and spatial scope in this case study. Considering that the AtLAST energy system is projected to be constructed in the 2030s, we set the year 2030 as the basis for component production and implement future power mixes of production areas accordingly. We determine specific likely production areas and include the transportation distances to the location of AtLAST's energy system to the environmental impact calculation. By utilizing up-to-date LCIs and regionalizing our LCA inputs based on assumed supply chains and electricity mixes in production countries in 2030, we depart from a black-box approach. We answer the research questions:

1. Which system has the lowest environmental impacts in the three impact categories considered?
2. What are the trade-offs between these three environmental impacts?
3. What is the regional distribution of these impacts?

2. Materials and Methods

2.1 Goal and Scope Definition

This comparative LCA aims to evaluate the environmental impacts of different off-grid energy system configurations for powering the new telescope AtLAST on the Chajnantor plateau in Chile. This plateau is the best site to perform sub-millimeter observations from ground, and as such it hosts more than ten international sub-mm/mm observatories, including the most powerful in the world. AtLAST is planned to be located near the Atacama Large Millimeter Array (ALMA) and the Atacama Pathfinder Experiment (APEX) at approximately 5,000m above sea level (Fig. 2).

This LCA study targets the decision makers for the new telescope AtLAST, next to energy system modelers, astronomers, and off-grid system operators interested in RES implementation. We follow the ISO14040:2006 and ISO14044:2006 standards (Technical Committee ISO/TC 207 2006; Technical Committee ISO/TC 207/SC 5 2006) and employ a comparative, attributional cradle-to-gate LCA. The aim is to identify the key activities within the life cycle of the off-grid energy systems and their components that contribute the most to environmental impacts (Guinée et al. 2018). Given the scope of the attributional assessment, we do not expect the decisions made for the telescope's energy system to have significant far-reaching consequences that would require consequential modeling. This may differ when conducting an LCA on a national or international energy system. The functional unit is defined as delivering annual power of 7.7GWh$_e$, based on the estimated demand curve of the telescope, over a lifetime of 25 years. The start of operation is defined as 2030. Techno-economic optimization details regarding the energy system, including the telescope's demand, component choices, and timeline, can be found in Viole et al. (2023b). Figure 3 shows the system boundary, which includes the production of components, their transport to the energy system site, and the operation and maintenance of the system.

Our life cycle impact assessment (LCIA) applies the Environmental Footprint (EF) 3.0 method, implemented in the SimaPro software (v9). From the EF's 16 environmental impact categories and their respective impact assessment models, we selected the three most relevant for the analysis of a remote energy system such as AtLAST, namely climate change, mineral resource depletion, and water use (see Table 1 for units and impact assessment models). The first two categories were chosen as current energy policies put much emphasis on climate change and the depletion of mineral resources. The environmental impact of water use is considered due to the location of the proposed energy system in a hyperarid desert. The median humidity at the APEX telescope, close to the potential AtLAST site, was 25% in 2022 (Atacama Pathfinder Experiment (APEX) 2023). The EF 3.0 method includes the AWARE (Available WAter REmaining) regionalised water scarcity footprint (Boulay et al. 2018). AWARE distributes regional weighting factors relating to the local water scarcity, e.g. Chile has a weighting factor of 81.37, Norway 0.76, and factors in China vary between 0.39 in Hunan and 87.07 in Hubei. That means that 1m^3 of water in Norway accounts for 0.76m^3 water eq of deprived water in the LCIA, while 1m^3 of Chilean water results in 81.37m^3 water eq.

2.2 Product systems and sizes: Energy system optimization

We consider four different energy system components: (1) a diesel generator, (2) a ground-mounted mono-crystalline silicon (mc-Si) PV park, (3) Lithium Iron Phosphate (LFP) batteries, and (4) a hydrogen storage system consisting of an alkaline electrolyzer (AE), compressed gas (CG) hydrogen storage and a proton-exchange membrane fuel cell (PEMFC). Different system compositions of these components can provide the energy required by the telescope according to the six scenarios described in the following. The components selection follows the technological feasibility on and nearby the Chajnantor plateau, as discussed in Viole et al. (2023b)'s techno-economic optimization. Here, we make some simplifications by a) only including on-site hydrogen production and b) focusing on systems located at a valley site of 2,500m altitude, at 23°02'S 68°06'W, supplying the telescope on the plateau via a 43km long subterranean power line (see Fig. 1). We exclude the option of an energy system at the telescope's site at 5,000m for operational reasons, such as the easier access for maintenance, less probability for snowfall, and more available building space.

The sizing of system components follows the GAMS-based techno-economic optimization highRES-AtLAST (Valenzuela Venegas 2022). Key features in the linear optimization are:

- Six scenarios allowing different system components to be built by the optimization model:

  a. Reference: Diesel generators

  b. PD: PV and diesel generators

  c. PDB: PV, diesel generators, and batteries

  d. PB: PV and batteries

  e. PDBH: PV, diesel generators, batteries, and hydrogen technology

  f. PBH: PV, batteries, and hydrogen technology
- The annual demand of the telescope, divided in one hour segments, is met without load shedding.
- To model hourly PV capacity factors, we apply the weather year 2020 from the ERA5 Reanalysis (Hersbach et al. 2020).
- We use 2030 as the year for costs and electricity demand.
- The optimization equation minimizes the annualized total costs of the system composed of investment and dispatch costs.

The resulting capacity and generation are reported in Table 2 and Fig. 4. The scenarios PDBH and PDB have the lowest LCOEs, while scenarios PB and PBH have the lowest direct GHG emissions. These direct emissions consist only of the diesel burned in the generators on site, applying an emission factor of 0.86t CO_2e/MWh (Gaete-Morales et al. 2018). PB and PBH scenarios require five times the amount of capacity installed compared to the reference scenario and generate more than double the electricity. The system curtails generation from PV when the solar generation exceeds the demand and the storage options.

2.3 Compilation of the life cycle inventories (LCI)

In this LCA, we include ground-mounted, mc-Si PV panels, LFP batteries, AE, CG hydrogen storage, PEMFC, and diesel generators, as the system components, connected to the telescope via subterranean AC power lines. The component selections in this LCA are driven by economic considerations while also taking into account their mineral resource impacts. We chose Li-ion over lead acid batteries due to their longer cycle life and reduced need for replacements. Within Li-ion battery chemistries, we opt for LFP batteries based on the findings of Yudhistra et al. (2022), which showed lower impacts on climate change and mineral resource depletion compared to other battery types like NMC (Nickel Manganese Cobalt) and lead acid ones. LFP batteries' cathodes consist of ~8% lithium, with the remaining composition mostly made up from iron and phosphorus (International Energy Agency 2022a). In the hydrogen system, we consider the more economical AE over PEM electrolyzers. For hydrogen storage, we apply CG due to its cost-effectiveness. Other storage options include liquid hydrogen, which is more expensive, underground storage (e.g. in salt caverns) better suitable for larger storage volumes, and storage in metal hydrides, not widely available yet (Egeland-Eriksen et al. 2021).

2.3.1 Production of system components

For the production LCIs, we use inventories published after 2015 wherever possible, adjusted to the temporal and regional scope of the work. In PV production, we refer to Frischknecht et al. (2020)'s LCIs, modifying the background processes to ecoinvent 3.7.1 datasets. This includes the production of PV cells, made from silicon wafers based on Czochralski single silicon crystals. PV modules are formed by connecting multiple PV cells. Regarding LFP batteries, we relied on Porzio and Scown (2021)'s LCI, which included a $LiFePO_4$-based cathode and a graphite-based anode. Additionally, we employed Quan et al. (2022)'s inventories for the production of $LiFePO_4$ from lithium carbonate and iron phosphate.

In the hydrogen system, LCIs are based on Koj et al. (2017) for the AE with a Zirkon membrane, on Boureima et al. (2011) and Wulf et al. (2018) for the steel-based CG hydrogen storage tank, and on Notter et al. (2015) and Weber et al. (2018) for the PEMFC with a Nafion membrane. The diesel-electric generating set and background datasets are taken from the ecoinvent database (v. 3.7.1). Detailed activity levels are available as an open-source dataset in Viole et al. (2023a).

Setting the temporal and regional scope

For this case study we choose specific production locations based on production assumptions for 2030. These locations impact the water use, power mixes, and shipping distances. For PV panels, the majority of shipments to Latin America in recent years originated from China, specifically Jiangsu and Xinjiang regions (International Energy Agency 2022b). It is not possible to determine the exact ratio between the two supplying regions. Therefore, we allocate these regions in a 50:50 proportion as our sourcing locations for PV panels. In batteries, China currently accounts for three quarters of the global Li-ion production and is expected to maintain a 70% production capacity share through 2030 (International Energy Agency 2022a). Cathode production for LFP batteries in China is distributed across various provinces, including Hunan, Yunnan and Hubei. We include these three regions as equal sourcing locations for the batteries in this work. For hydrogen systems, manufacturers today are in the process of scaling up their capacities. Europe houses the main MW-scale AE producers, such as NEL Hydrogen in Norway, Sunfire in Germany, and John Cockerill in France, while the latter also has some production in Jiangsu in China (John Cockerill; Nel Hydrogen; Sunfire). PEMFC production of stationary fuel cells applicable for AtLAST's energy system is conducted by Plug Power in New York State, USA and by PowerCell in Sweden (Plug Power 2022; PowerCell 2022). In our LCA, we implement Herøya, Norway as the production location for AE, and Slingerland, NY, USA for PEMFC. Local CG storage production is available in Chile. We accounted for 43km of 24kV underground power lines to connect the power plant at 2,500m altitude with the telescope at 5,000m, and adapted Arvesen et al. (2015)'s LCI for 22kV subterranean distribution lines to a production facility in Chile.

We include region-specific electricity mixes for 2030 in the LCIs. For the Chinese production sites, we use a global Chinese power mix following energy system optimizations from Zhang et al. (2022). We could not use regionally varying power mixes for the different Chinese production locations due to the continuous increasing of the Chinese targets of renewable shares. Regional power mix calculations like Shen et al.'s from (2019) fall far short of the most conservative assumptions in renewables expansion by Zhang et al. from (2022), hence we include the latter country-wide national power mixes, which assume a carbon-neutral power generation share of 54% in 2030, including RES and nuclear power. For the Chilean and US-American power mixes in 2030, we follow the National outlines of RES integration for 2030 based on Ministerio de Energía, Gobierno de Chile (2020) and, for Norway we adapt DNV (2022)'s 2030 forecast.

To understand local circumstances relevant for AtLAST, the authors visited APEX, a 12-m single-dish telescope on Chajnantor, in 2022. Learnings like common practises in PV cleaning and staff commuting are fed into the assumptions for the energy systems' LCA, which we shall discuss in the next section.

2.3.2 Transport of components to site, operation and maintenance

We estimate transportation routes between the production places and the energy system's site based on common shipping routes and streets, where goods are mainly shipped to the Antofagasta port and then lorried to the site, see Table 6 in appendix. We apply ecoinvent 3.7.1 datasets to integrate transportation by train, lorry and containership. The operation and maintenance of the energy system for AtLAST includes the fuels burned by the system´s components during operation, the travels of the maintenance personnel to and from the site, the PV cleaning and component replacements.

Maintenance workers

To estimate travels of the maintenance crew, we conducted qualitative interviews with observatory operators from APEX during 2022. Scaling up the operations of this 12m to our prospective 50m-dish telescope, we foresee the need for three workers on duty for maintenance of the system, with two in day-shift, and one in night-shift. In the operation of telescopes in the Atacama, personnel typically fly in for 8 day-shifts, after which they fly home and are off-duty for 6 days. In the LCI for the maintenance workers, we include one return-trip from Santiago de Chile to the energy system site per week per worker. We account a third of the energy system workers' shift and commuting emissions towards the energy system, as these engineers hold other duties, e.g. technical handling of astronomical instrumentation.

Replacements

Further in maintenance, we include the necessary replacements over the system's lifetime, as given in Table 3. For the PV degradation, we choose a higher value than the commonly used 0.5-0.8%/year (yr), as we are operating in arid desert conditions, which leads to soiling. Additionally, high ultraviolet (UV) irradiation is present in the Atacama, typically ~40% above the annual UV-B doses in Northern Africa (Cordero et al. 2018). High UV exposure can lead to encapsulant discoloration, which lowers the output power. Field studies in deserts report degradation rates ranging from 0.74 ± 0.29%/yr for poly-crystalline silicon (pc-Si) panels under maritime desert conditions (Hassan Daher et al. 2022), 0.15-2.83%/yr for pc-Si in the Atacama (Vásquez et al. 2021), 1.89%/yr for mc-Si panels in the Sahara (Bouraiou et al. 2015), to 1.25-4.22%/yr in pc-Si panels operated in a hot semi-arid climate (Bansal et al. 2022).

We implement 1.56%/yr of degradation as the average over these studies' median values. This requires adding 8% of total PV capacity every 5 years to offset the degraded modules. In the lifetime for the batteries, AE and PEMFC, we attribute 290 cycles/yr for the batteries, 3,400 operation hours/yr for AE stacks and 5,000h/yr for PEMFC and follow the US DOE's estimated component lifetimes (Viswanathan et al. 2022).

Photovoltaic cleaning

In operating PV parks in the Atacama Desert, Vásquez et al. (2021), found soiling as the most frequent problem, since layers of dust on the panels reduce their power output. To reduce soiling, common cleaning options include natural cleaning by wind and rain, manual cleaning with water and cleaning robots. We follow the declarations of the operators of the PV installations of the Energy Cooperative of San Pedro the Atacama (CESPA) to assume that PV Arrays are cleaned twice a year, and include biannual manual cleaning with mild detergent and solar cleaning brushes in our maintenance LCI, assuming the need for 0.5L deionized water per m^2 of panel cleaned (Kazem et al. 2020).

Water usage of the hydrogen system

Proposing hydrogen storage systems in a desert leads to questions related to water use. San Pedro de Atacama has access to brackish water with ~2.3% salt content. In calculations for the desalination and deionization of the water for the hydrogen system and the PV cleaning, we account for water losses of 27% in the reverse osmosis desalination and 20% in the deionization (GHD 2022; Chululo - Revista Informativa de la Comuna de San Pedro de Atacama 2022). The proposed hydrogen system uses 9L of deionized water to produce 1kg hydrogen (H_2). We include losses in the AE of 1L water/kg H_2 produced, 15% H_2 lost during compression and storage, 13% H_2 lost in purging of the PEMFC (Esbo et al. 2020).

The water needs for scenarios PDBH and PBH are calculated with 205 and 323 m^3/yr of deionized water, respectively, or 352 and 553m^3 of brackish water extracted at the local sources, respectively (see Supplementary Material). These numbers do not justify the need of an own desalination unit in our case, hence the usage of a local desalination plant with 1.9kWh/m^3 water desalinated is included in the LCI (Antonyan 2019; Cetinkaya and Bilgili 2019), where the energy stems from a local PV and battery park.

3. Results and discussion

We compare the environmental impacts of the six energy system scenarios over a 25-year lifetime, see absolute values in Table 4. To visualize the results, Fig. 5 shows relative values to the maximum value in the impact category. The climate change impacts are set relatively to the CO_2e emissions of the reference scenario, which holds most emissions over the system's lifetime. Scenario PB shows the lowest GHG impact across the life cycle, by solely supplying AtLAST with energy from PV and batteries. At the same time, this scenario has the greatest impact in mineral resource depletion. The highest impact in water use is seen in scenario PBH, which has the second-lowest climate change impact. There are trade-offs between the three impact categories, as each scenario has its own strengths and weaknesses in terms of environmental impact.

3.1 Life cycle GHG emissions

The scenarios' GHG emissions can be broken down into the contribution of production, transportation, operation and maintenance steps (Fig. 6). In the reference scenario, most life cycle GHG emissions are made up by direct emissions during the operation phase, where diesel generates all the power needed by the telescope. Adding PV panels to this system, scenario PD, lowers these direct emissions by 41%. The production phase now includes slightly more emissions, mostly due to the manufacturing of PV panels. Over the considered life cycle, the PD scenario lowers the GHG emissions by 39% compared to the reference scenario.

3.1.1 Running diesel as backup - Scenarios PDB and PDBH

Scenarios PDB and PDBH, which use mostly RES and run diesel generators as backup, reduce life cycle CO_2e by 87%, compared to the reference scenario. The detailed distribution of relative GHG emissions in scenario PDB is shown in Fig. 7. The diesel burned to supply 7% of the annual demand in this scenario makes up 50% of this system's emissions, while the production of the RES, PV panels and batteries, supplying the other 93% of the telescope's demand, account for another 47% of the total emissions. The scenarios PDB and PDBH reach life cycle carbon intensities of 0.115 and 0.113kg CO_2e/kWh, respectively (Table 4). Over the 25-year life cycle, the GHG emissions for replacements, which make up 15% of the life cycle GHG emissions, are about half the size of the initial installation's GHG emissions. Both the transport of the components from production sites to the Atacaman location and staff commuting of the maintenance personnel have a rather miniscule influence.

3.1.2 Systems with 100% RES - scenarios PB and PBH

Scenario PB, one of the two 100% RES scenarios, has the overall lowest life cycle GHG impact, consisting of 0.077kg CO_2e/kWh supplied. Compared to PDB, we see an increase in emissions from PV and battery production by 40% and 51%, respectively (Fig. 6). This is interlinked with the higher capacities built in this scenario, as the PV and battery system must supply the telescope throughout the given weather year, that is also during multiple days of cloudiness, without having a diesel generator as backup. However, the upstream emissions from these larger capacities do not exceed the evaded CO_2e emissions from diesel burned. Hence this scenario's life cycle GHG emissions are the overall lowest in this study.

When we add a hydrogen system into the mix, that is scenario PBH, slightly higher GHG emissions are present, as the production of a second energy storage technology has to be included. At 0.080kg CO_2e/kWh, PBH is the scenario with the second-lowest life cycle GHG emissions out of the six scenarios compared.

3.2 Water use

In the renewable energy systems' life cycle water use, a high impactor is the PV panel production, accounting for 1.3 (PD) to 3.5 (PBH) million m^3 water eq, see Fig. 8. This relates to 44-57% of the scenarios' total water use. Moreover, the battery production makes for 1.8 (PDBH) to 3.7 (PB) million m^3 water eq, a share of 31-49% of the scenarios' total water use. In the upstream processes, especially the Czochralski process in the PV production and the phosphoric acid production for the LFP cathode material push up the water use. The water use on site in the Atacama during operation and maintenance, depicted with an 'o' hatch in Fig. 8, mainly comprises water for the hydrogen system. This accounts for 0.4-0.6 million m^3 water eq, that is 16,500-26,000m^3 water eq/yr. Compared to the water used in PV cleaning, the hydrogen systems have about 15 times the impact. The water use for the hydrogen system's operation had a share of 7-8% in the systems where hydrogen was included.

3.3 Mineral resource depletion

In mineral resource depletion, we find a positive correlation between the size of RES capacities built and the associated environmental impact, see Fig. 9. The relative mineral resource flow of scenario PDBH is depicted in Fig. 10. Most of the mineral resource impact stemmed from the mining of copper and silver. Copper is needed in the production of batteries and PV panels, as it is used in the current collector of the battery's anode and the wires and cell interconnections of solar panels. PV additionally requires silver as part of the metallization paste applied on the wafers for electric contacts. Hydrogen systems contribute to the mineral resource depletion with the use of platinum in PEMFCs. These used resources are weighed to kg Sb eq in the EF 3.0 method with factors of $1.37 \cdot 10^{-3}$ (copper), 2.22 (platinum), and 1.18 (silver). Lithium, with a weighting factor of $1.15 \cdot 10^{-5}$, accounts for only up to 0.013% of the mineral resource depletion in the compared systems. The share of battery and PV production far outweighs any other influence on the mineral resource depletion.

According to the EU's foresight study on critical raw materials, the materials used in AtLAST's energy systems are categorized from low to moderate supply risks. Natural graphite, which is not considered in EF 3.0's mineral depletion assessment, is ranked with a moderate supply risk. Lithium, titanium and silicon metal have low supply risks, while nickel and copper have very low risks. Although materials like lithium are not currently considered scarce, possibilities of future scarcities emerge as demand continues to grow. The EU has projected a significant increase in lithium demand, estimating a multiplication factor between 8 and 18 from the year 2020 to 2030 (European Commission. Directorate General for Internal Market, Industry, Entrepreneurship and SMEs. 2020). Compared to this general overview of supply risks, the resource and mineral depletion impact assessment of this work showed rather low numbers. It is however important to note that emerging scarcities in graphite and lithium could potentially alter these results for batteries in the mid-term future.

3.4 Trade-offs in combining energy system components

Trade-offs between the assessed environmental impacts are unavoidable. The reference scenario with the overarching highest CO_2e emissions had the smallest impact in water use and mineral depletion. Scenarios that significantly decrease the carbon intensity of the power supplied to the telescope entailed the usage of energy storage systems, either batteries or a HESS with batteries and a hydrogen storage system. Scenarios with solely batteries resulted in slightly higher mineral depletion, those with HESS had higher water use. The biggest impactor in mineral resource use and water use was the PV park size. Its initial capacities ranged between 2.5 and 6.5 MWp, depending on scenario setup, where the larger capacities were present in 100% RES scenarios.

3.5 Global distribution of environmental impacts

While this work compares the life cycle impacts of an off-grid energy system to operate in Chile, the sourcing locations of minerals, and the impacts during the production and transportation phase are distributed globally. Fig. 11 shows the global distribution of climate change and water use impact, and Fig. 12 maps out the shares of mineral resource depletion. Note that the global water use in the reference scenario resulted in a negative value, as in the background data some water is extracted on country-level, but released back on a Global/Rest-of-the-World level.

Comparing the global distribution of environmental impacts, we can see a shift in impacts depending on the share of RES. The highest climate change impact in Chile takes place in the reference scenario, stemming from the diesel burned in the generators. The less diesel we use in the energy systems, the lower the Chilean climate change impact. Apart from this, GHG emissions are mainly accounted as Rest-of-the-World and Global (both depicted as Global in Fig. 11), that is without a specific country-affiliation. In water use, the reference case mainly accounts the upstream of the diesel production, e.g. in the Middle East. When using systems with RES, the water use in energy system component production globally and in China rises. We can clearly see the impact of the hydrogen system with its distributed water use in Chile in scenarios PDBH and PBH, while scenarios with PV and batteries solely have the water use for the PV cleaning to account for in Chile. The mineral resource depletion of the compared energy system scenarios follows the underlying share of sourcing locations for minerals in ecoinvent. Big shares in this environmental impact category are held by Chile, which serves as a source for copper and silver, China for copper, and South Africa and Russia for platinum. Copper, which had the bear share in this impact category in this study, is further sourced from Russia, Australia, and North America, amongst others.

3.6 Sensitivity analysis

In the comparative LCA conducted, we found two important contributors to the climate change impacts: 1) the assumed 2030 power mixes in the Chinese production areas of PV panels and LFP batteries, and 2) the battery replacements, the impact of which could be sensitive to the replacement rates.

To test the sensitivity of our results given different power mixes in 2030-China, we change them towards a slower and a faster transition towards carbon-neutral power supply (includes both RES and nuclear generation). The lower boundary is set with a share of 35.5% in carbon-neutral generation, applying the unaltered Chinese power mix from 2021 (China electricity council 2023). Our reference case in the study (called reference transition in Table 5) had applied a share of 54% (Zhang et al. 2022). The upper boundary is set with a power mix where GHG emissions in China peak in 2025, with a carbon-neutral generation share of 64.9% (Zhang and Chen 2022). We find that by applying these power mixes, the life cycle GHG impact of our energy systems deviates by -2.8%/+6.0%, see Table 5. Changes in the power mix affect scenario PB the most, as it has the highest battery capacity built.

Continuing with testing the sensitivity of the battery-related assumptions in this work, we change the battery replacement rates in the LCA. These replacements were a main contributing factor in all three environmental impact categories. We had set the original replacement rates of the LFP batteries at every 2,640 cycles and 2.7 replacements over 25 years (see assumptions in Table 3, Visnawanathan et al. (2022)'s assumption for 2030). In studying their sensitivity, we change these rates to the lower boundary at every 15 years and 1.7 replacements over 25 years (Cole et al. (2021)'s not-cycle specific lifetime), and the upper boundary at every 2,400 hours and 3.3 replacements over 25 years (Visnawanathan et al. (2022)'s assumption for 2021).

Fig. 13 shows the relative changes in environmental impacts given the boundary replacement rates. We see changes in the climate change impacts by up to -13%/+5%, with scenario PB again affected the most, as it contains most battery capacity. Different replacement rates in batteries have the strongest effect on the mineral resource depletion, with relative changes up to -30%/+10%. The water use deviates up to -19%/+7%.

3.7 Comparing the carbon footprints of the energy system with the construction of the 50m-dish telescope

The climate change impacts of space activities and astronomy have come to the foreground in recent years, for one with recent touristic space missions of the very rich, but also with debates around the carbon footprint of astronomers, whose need for telescopes results in median carbon intensities of 22 (space observatories) and 24tCO_2e (ground-based observatories) per scientific paper (Stevens et al. 2020; Frischknecht et al. 2020; Ryan et al. 2022). To put our energy system LCA for the AtLAST telescope into perspective, we compare its life cycle climate change impact to the rough estimation of the CO_2e impact of building the telescope itself. Knödlseder found monetary emission factor for ground-based observatories at 1,700-1,800t CO_2e /M€, where their need for concrete and steel were the biggest contributor (2022). First cost estimates for AtLAST account for a construction budget of 250-300M€, resulting in roughly 425,000-540,000t CO_2e, provided the technological production of steel and concrete remains the same. The 14,700 to 107,600t of lifetime CO_2e emissions calculated for the renewable power scenarios in this work compare with 3 to 25% of the projected telescope's construction GHG impact.

4. Possibilities to expand this LCA

This work presents a cradle-to-gate comparative LCA on various off-grid energy systems in Chile using components from selected production regions. As such, it is subject to various limitations and opens up opportunities for future work. Our scope was specific to certain locations and timeframes, incorporating LCIs of future power mixes in production and transportation routes. If we selected other locations than China (for PV, batteries), the USA (for PEMFC), Norway (for AE) and Chile (for other components), the environmental impacts of the respective energy systems for AtLAST would differ. Faster or slower transitions towards RES in the production areas' power mixes can further lead to varying results. By applying a sensitivity analysis, we could address some of these uncertainties and show that the climate change impact varies by up to -2.7/+6.4% with lower and upper boundary carbon-neutral generation shares in the 2030 Chinese power mix. When using upper and lower boundaries in battery replacement assumptions, the GHG emissions change up to -13%/+5%.

Regarding future work, the life cycle GHG emissions from this LCA shall be integrated into the techno-economical analysis for a multi-objective optimization considering both CO_2e emissions and LCOEs. This allows for finding the Pareto front between the lowest LCOE and lowest GHG emissions to supply the telescope (Konak et al. 2006). We can further conduct a similar study on the currently installed capacities supplying energy to the other observatories on Chajnantor, to help understand if an energy transition of all these telescopes would make sense environmentally, also regarding the expected lifetime remaining of the respective observatories. Options such as substituting the fossil diesel in the PDB or PDBH scenario with sustainable biodiesel could also be looked upon there.

To further advance the LCA community in the field of energy systems, it would be beneficial to reduce our reliance on black-box inputs such as ecoinvent datasets from 2009. Instead, we should strive to incorporate temporal and regional realities into our LCIs. This approach would significantly enhance the accuracy and relevance of our studies, leading to more reliable and insightful findings. This work showcased that applying more up-to-date LCIs than the ones available in ecoinvent can be done, though the literature search and implementation in SimaPro can be a tedious process. To ease the path for upcoming studies on energy system LCAs, we publish the LCIs applied in this work as detailed activity level datasets in Viole et al. (2023a).

5. Conclusions

With this comparative LCA we demonstrate that the production of RES components, especially PV panels and batteries, next to the burning of diesel in generators has the biggest impact on the CO_2e emissions over the life cycle of off-grid energy systems supplying a telescope in the Atacaman desert. Other operations, maintenance, and the transport of components to the site, in comparison, have minor impacts. Regarding our three research questions, we find the following.

The system with the lowest environmental impact in the three impact categories considered

We show that depending on the choice of components for the off-grid system, trade-offs between our three environmental impacts must be made, which are climate change, water use, and mineral resource depletion. The four scenarios with high shares in RES have emissions of 0.077-0.115kg CO_2e/kWh supplied, compared to GHG emissions of 0.559kg CO_2e/kWh when combining PV with diesel, and 0.917kg CO_2e/kWh employing only diesel generation in the reference scenario. This reference scenario has the lowest impact in both mineral resource depletion and water use, as these two impact categories are mainly impacted by RES components.

Trade-offs between the environmental impacts

Due to the desertic location of the energy system for the telescope AtLAST, this case study paid special attention to the water use. We find that over the life cycle, the water use of the production of PV panels and batteries in China has a much higher impact compared to the water use for the hydrogen production or the PV cleaning in the Atacama. The hydrogen system at most made up for 8% of the water use impact. We find systems with hydrogen storage to have a slightly higher water use than their counterparts with only batteries.

The mineral resource use is highly impacted by the required capacities of both PV panels and batteries. The highest impact in this category stems from copper, zinc, silver and titanium. Lithium, often cited as a scarce commodity for the expansion in battery production, has a minuscule share in this impact category, due to its low characterisation factor in the applied ADP method. This result is in line with the EU projections, which foresee a low supply risk for lithium. We find that systems with a HESS using hydrogen and batteries have a lower impact in this category than the systems only applying batteries as energy storage.

In trade-offs between the impact categories, we find that the systems with the lowest GHG emissions, the 100% RES ones, have the highest impact in water use and mineral resource depletion. The high-renewable scenarios have slightly higher GHG emissions, however their water and mineral resource use lies around 27% below that of the 100% RES scenarios. This is due to the smaller PV and storage capacities that they require.

Regional distribution of the environmental impacts

In assessing the regional distribution of the impacts, we find them localized in Chile in the reference scenario with solely diesel generators, and spread out much over the globe when applying RES, which largely are produced in China from mineral resources sourced all over the globe. The water use impact is located at the production facilities as well as on site in Chile for the PV cleaning and hydrogen system.

This work shows that lowering the environmental impact like for example GHG emissions in off-grid remote energy systems is a challenging task. Replacing the business-as-usual diesel generators with 100% RES lowers the GHG intensity per kWh supplied, while trade-offs in mineral depletion and water use have to be taken. We show that a variety of energy systems with high shares of RES could be deployed to power the planned telescope, and that systems with some fossil generation next to high shares of renewables can evade oversizing of components, thus saving on resources and have a higher security of supply. Given the high importance that telescope operators put on power quality, the authors recommend hybrid energy systems combining renewables, energy storage systems and conventional power generators for use in the mid-term future.

Declarations

Author contributions

Conceptualization: Isabelle Viole, Li Shen; Methodology: Isabelle Viole, Li Shen; Formal analysis and investigation: Isabelle Viole, Luis Ramirez Camargo; Writing - original draft preparation: Isabelle Viole; Writing - review and editing: Li Shen, Luis Ramirez Camargo, Marianne Zeyringer, Sabrina Sartori; Funding acquisition: Sabrina Sartori, Isabelle Viole; Resources: Li Shen; Supervision: Li Shen, Marianne Zeyringer, Luis Eduardo Ramirez Camargo, Sabrina Sartori.

Conflicts of Interest

The authors declare no conflict of interest.

Data availability statement

The life cycle inventories generated during the current study are available in the Zenodo repository, https://doi.org/10.5281/zenodo.8026737. (We will make these datasets available as open source when this paper is published.)

Acknowledgments

This project has received funding from the European Union’s Horizon 2020 research and innovation programme under grant agreement No. 951815 (AtLAST project). Isabelle Viole acknowledges internationalization support from UiO:Life Science and from UiO:Energy and Environment for this work. Li Shen and Luis Ramirez Camargo’s contributions were funded by the Copernicus Institute of Sustainable Development, Utrecht University. We thank Claudia Cicone from the Institute of Theoretical Astrophysics, University of Oslo, for valuable input.

References

1. Antonyan M (2019) Energy Footprint of Water Desalination. Master Thesis, University of Twente
2. Arvesen A, Hauan IB, Bolsøy BM, Hertwich EG (2015) Life cycle assessment of transport of electricity via different voltage levels: A case study for Nord-Trøndelag county in Norway. Applied Energy 157:144–151. https://doi.org/10.1016/j.apenergy.2015.08.013

3. Atacama Pathfinder Experiment (APEX) (2023) Weather data - Humidity 2022 at APEX telescope. https://www.apex-telescope.org/apex-dashboard/d/MQgvc4Onz/historical-weather. Accessed 8 May 2023
4. Bansal N, Jaiswal SP, Singh G (2022) Prolonged degradation and reliability assessment of installed modules operational for 10 years in 5 MW PV plant in hot semi-arid climate. Energy for Sustainable Development 68:373–389. https://doi.org/10.1016/j.esd.2022.04.008
5. Barros MV, Salvador R, Piekarski CM, et al (2020) Life cycle assessment of electricity generation: a review of the characteristics of existing literature. Int J Life Cycle Assess 25:36–54. https://doi.org/10.1007/s11367-019-01652-4
6. Berrill P, Arvesen A, Scholz Y, et al (2016) Environmental impacts of high penetration renewable energy scenarios for Europe. Environ Res Lett 11:014012. https://doi.org/10.1088/1748-9326/11/1/014012
7. Bilich A, Langham K, Geyer R, et al (2017) Life Cycle Assessment of Solar Photovoltaic Microgrid Systems in Off-Grid Communities. Environ Sci Technol 51:1043–1052. https://doi.org/10.1021/acs.est.6b05455
8. Bocklisch T (2015) Hybrid Energy Storage Systems for Renewable Energy Applications. Energy Procedia 73:103–111. https://doi.org/10.1016/j.egypro.2015.07.582
9. Boulay A-M, Bare J, Benini L, et al (2018) The WULCA consensus characterization model for water scarcity footprints: assessing impacts of water consumption based on available water remaining (AWARE). Int J Life Cycle Assess 23:368–378. https://doi.org/10.1007/s11367-017-1333-8
10. Bouraiou A, Hamouda M, Chaker A, et al (2015) Analysis and evaluation of the impact of climatic conditions on the photovoltaic modules performance in the desert environment. Energy Conversion and Management 106:1345–1355. https://doi.org/10.1016/j.enconman.2015.10.073
11. Boureima F-S, Wynen V, Sergeant N, et al (2011) CLEVER Clean Vehicles Research: LCA and Policy Measures. LCA report. Belgian Science Policy, Brussels, Belgium
12. Cetinkaya AY, Bilgili L (2019) Life Cycle Comparison of Membrane Capacitive Deionization and Reverse Osmosis Membrane for Textile Wastewater Treatment. Water Air Soil Pollut 230:149. https://doi.org/10.1007/s11270-019-4203-0
13. China electricity council (2023) 2021/ Electricity generation statistics 2021. China electricity council, Beijing, China
14. Chululo - Revista Informativa de la Comuna de San Pedro de Atacama (2022) A fin de año esperan habilitar planta de agua potable en San Pedro de Atacama. https://www.chululo.cl/pages/recortes2.php?id=10072022_025743. Accessed 16 Jan 2023
15. CML (2016) CML-IA Characterisation Factors - Leiden University. https://www.universiteitleiden.nl/en/research/research-output/science/cml-ia-characterisation-factors. Accessed 22 Jun 2023
16. Cole W, Frazier AW, Augustine C (2021) Cost Projections for Utility- Scale Battery Storage: 2021 Update. National Renewable Energy Laboratory, Golden, CO

17. Come Zebra EI, van der Windt HJ, Nhumaio G, Faaij APC (2021) A review of hybrid renewable energy systems in mini-grids for off-grid electrification in developing countries. Renewable and Sustainable Energy Reviews 144:111036. https://doi.org/10.1016/j.rser.2021.111036
18. Cordero RR, Damiani A, Jorquera J, et al (2018) Ultraviolet radiation in the Atacama Desert. Antonie van Leeuwenhoek 111:1301–1313. https://doi.org/10.1007/s10482-018-1075-z
19. DNV (2022) Energy Transition Norway 2022. A national forecast to 2050. Høvik, Norway
20. Egeland-Eriksen T, Hajizadeh A, Sartori S (2021) Hydrogen-based systems for integration of renewable energy in power systems: Achievements and perspectives. International Journal of Hydrogen Energy 46:31963–31983. https://doi.org/10.1016/j.ijhydene.2021.06.218
21. Endo N, Shimoda E, Goshome K, et al (2019) Simulation of design and operation of hydrogen energy utilization system for a zero emission building. International Journal of Hydrogen Energy 44:7118–7124. https://doi.org/10.1016/j.ijhydene.2019.01.232
22. Esbo MR-, Ranjbar AA, Rahgoshay SM (2020) Analysis of water management in PEM fuel cell stack at dead-end mode using direct visualization. Renewable Energy 162:212–221. https://doi.org/10.1016/j.renene.2020.06.078
23. European Commission. Directorate General for Internal Market, Industry, Entrepreneurship and SMEs. (2020) Critical raw materials for strategic technologies and sectors in the EU: a foresight study. Publications Office, LU
24. Frischknecht R, Stolz P, Krebs L, et al (2020) Life Cycle Inventories and Life Cycle Assessments of Photovoltaic Systems. International Energy Agency (IEA), France, Paris
25. Gaete-Morales C, Gallego-Schmid A, Stamford L, Azapagic A (2018) Assessing the environmental sustainability of electricity generation in Chile. Science of The Total Environment 636:1155–1170. https://doi.org/10.1016/j.scitotenv.2018.04.346
26. Gandiglio M, Marocco P, Bianco I, et al (2022) Life cycle assessment of a renewable energy system with hydrogen-battery storage for a remote off-grid community. International Journal of Hydrogen Energy 47:32822–32834. https://doi.org/10.1016/j.ijhydene.2022.07.199
27. GHD (2022) Water for Hydrogen. https://www.ghd.com/en/perspectives/water-for-hydrogen.aspx. Accessed 15 May 2023
28. Ghenai C, Salameh T, Merabet A (2020) Technico-economic analysis of off grid solar PV/Fuel cell energy system for residential community in desert region. International Journal of Hydrogen Energy 45:11460–11470. https://doi.org/10.1016/j.ijhydene.2018.05.110
29. Guinée JB, Cucurachi S, Henriksson PJG, Heijungs R (2018) Digesting the alphabet soup of LCA. Int J Life Cycle Assess 23:1507–1511. https://doi.org/10.1007/s11367-018-1478-0
30. Guinée JB, Heijungs R (1995) A proposal for the definition of resource equivalency factors for use in product life-cycle assessment. Environ Toxicol Chem 14:917–925. https://doi.org/10.1002/etc.5620140525
31. Hassan Daher D, Gaillard L, Ménézo C (2022) Experimental assessment of long-term performance degradation for a PV power plant operating in a desert maritime climate. Renewable Energy 187:44–

55. https://doi.org/10.1016/j.renene.2022.01.056
32. Hersbach H, Bell B, Berrisford P, et al (2020) The ERA5 global reanalysis. Quarterly Journal of the Royal Meteorological Society 146:1999–2049. https://doi.org/10.1002/qj.3803
33. Hertwich EG, Gibon T, Bouman EA, et al (2015) Integrated life-cycle assessment of electricity-supply scenarios confirms global environmental benefit of low-carbon technologies. Proc Natl Acad Sci USA 112:6277–6282. https://doi.org/10.1073/pnas.1312753111
34. HyResource (2020) Sir Samuel Griffith Centre. In: HyResource. https://research.csiro.au/hyresource/sir-samuel-griffith-centre/. Accessed 15 May 2023
35. International Energy Agency (2022a) Global Supply Chains of EV Batteries. OECD, Paris
36. International Energy Agency (2022b) Special Report on Solar PV Global Supply Chains. OECD, Paris
37. IPCC (2013) Climate Change 2013: The Physical Science Basis. Contribution of Working Group I to the Fifth Assessment Report of the Intergovernmental Panel on Climate Change. Cambridge University Press, Cambridge, United Kingdom and New York, NY, USA
38. John Cockerill Manufacturing Facilities. In: Green Hydrogen - John Cockerill. https://h2.johncockerill.com/en/manufacturing-facilities/. Accessed 14 Feb 2023
39. Kazem HA, Chaichan MT, Al-Waeli AHA, Sopian K (2020) A review of dust accumulation and cleaning methods for solar photovoltaic systems. Journal of Cleaner Production 276:123187. https://doi.org/10.1016/j.jclepro.2020.123187
40. Klaassen PD, Mroczkowski TK, Cicone C, et al (2020) The Atacama Large Aperture Submillimeter Telescope (AtLAST). In: Ground-based and Airborne Telescopes VIII. SPIE, pp 544–563
41. Knödlseder J, Brau-Nogué S, Coriat M, et al (2022) Estimate of the carbon footprint of astronomical research infrastructures. Nature Astronomy. https://doi.org/10.1038/s41550-022-01612-3
42. Koj J, Wulf C, Schreiber A, Zapp P (2017) Site-Dependent Environmental Impacts of Industrial Hydrogen Production by Alkaline Water Electrolysis. Energies 10:860. https://doi.org/10.3390/en10070860
43. Konak A, Coit DW, Smith AE (2006) Multi-objective optimization using genetic algorithms: A tutorial. Reliability Engineering & System Safety 91:992–1007. https://doi.org/10.1016/j.ress.2005.11.018
44. McCallum CS, Kumar N, Curry R, et al (2021) Renewable electricity generation for off grid remote communities; Life Cycle Assessment Study in Alaska, USA. Applied Energy 299:117325. https://doi.org/10.1016/j.apenergy.2021.117325
45. Ministerio de Energía, Gobierno de Chile (2020) Carbono Neutralidad en el Sector Energía. Proyección de consumo energético nacional 2020. Ministerio de Energía, Gobierno de Chile, Santiago de Chile
46. Nel Hydrogen Atmospheric Alkaline Electrolyser. In: Nel Hydrogen. https://nelhydrogen.com/product/atmospheric-alkaline-electrolyser-a-series/. Accessed 14 Feb 2023
47. Notter DA, Kouravelou K, Karachalios T, et al (2015) Life cycle assessment of PEM FC applications: electric mobility and μ-CHP. Energy Environ Sci 8:1969–1985. https://doi.org/10.1039/C5EE01082A

48. Odou ODT, Bhandari R, Adamou R (2020) Hybrid off-grid renewable power system for sustainable rural electrification in Benin. Renewable Energy 145:1266–1279. https://doi.org/10.1016/j.renene.2019.06.032
49. Olabode OE, Ajewole TO, Okakwu IK, et al (2021) Hybrid power systems for off-grid locations: A comprehensive review of design technologies, applications and future trends. Scientific African 13:e00884. https://doi.org/10.1016/j.sciaf.2021.e00884
50. Plug Power (2022) Plug Power Ramping Up its New Slingerlands Fuel Cell Factory - Plug Power. https://www.plugpower.com/in_the_news/plug-power-ramping-up-its-new-slingerlands-fuel-cell-factory/. Accessed 14 Feb 2023
51. Porzio J, Scown CD (2021) Life-Cycle Assessment Considerations for Batteries and Battery Materials. Advanced Energy Materials 11:2100771. https://doi.org/10.1002/aenm.202100771
52. PowerCell (2022) Fuel Cell Systems – PowerCell Group. https://powercellgroup.com/fuel-cell-systems/. Accessed 14 Feb 2023
53. Quan J, Zhao S, Song D, et al (2022) Comparative life cycle assessment of LFP and NCM batteries including the secondary use and different recycling technologies. Science of The Total Environment 819:153105. https://doi.org/10.1016/j.scitotenv.2022.153105
54. Ramasawmy J, Klaassen PD, Cicone C, et al (2022) The Atacama Large Aperture Submillimetre Telescope: key science drivers. In: Zmuidzinas J, Gao J-R (eds) Millimeter, Submillimeter, and Far-Infrared Detectors and Instrumentation for Astronomy XI. SPIE, Montréal, Canada, p 9
55. Ringkjøb H-K, Haugan PM, Nybø A (2020) Transitioning remote Arctic settlements to renewable energy systems – A modelling study of Longyearbyen, Svalbard. Applied Energy 258:114079. https://doi.org/10.1016/j.apenergy.2019.114079
56. Rodríguez F (2022) ESO's Paranal Observatory starts receiving energy from the largest solar plant in Chile dedicated to astronomy. In: www.eso.org. https://www.eso.org/public/announcements/ann22010/. Accessed 13 Jul 2022
57. Ryan RG, Marais EA, Balhatchet CJ, Eastham SD (2022) Impact of Rocket Launch and Space Debris Air Pollutant Emissions on Stratospheric Ozone and Global Climate. Earth's Future 10:. https://doi.org/10.1029/2021EF002612
58. Shen W, Han W, Wallington TJ, Winkler SL (2019) China Electricity Generation Greenhouse Gas Emission Intensity in 2030: Implications for Electric Vehicles. Environ Sci Technol 53:6063–6072. https://doi.org/10.1021/acs.est.8b05264
59. Stevens ARH, Bellstedt S, Elahi PJ, Murphy MT (2020) The imperative to reduce carbon emissions in astronomy. Nat Astron 4:843–851. https://doi.org/10.1038/s41550-020-1169-1
60. Sunfire Hydrogen. The renewable Feedstock and energy carrier. In: Sunfire. https://www.sunfire.de/en/hydrogen. Accessed 14 Feb 2023
61. Tannous S, Besseau R, Prieur-Vernat A, et al (2019) A parameterized model for the estimation of life cycle environmental impacts of crystalline PV systems. Marseille, France

62. Technical Committee ISO/TC 207 (2006) ISO 14040. Environmental Management — Life Cycle Assessment — Principles and Framework. International Standard Organization, Geneva, Switzerland
63. Technical Committee ISO/TC 207/SC 5 (2006) ISO 14044. Environmental Management — Life Cycle Assessment — Requirements and Guidelines. International Standard Organization, Geneva, Switzerland
64. Valenzuela Venegas GA (2022) highRES-AtLAST. Power system optimization model for AtLAST telescope. https://github.com/highRES-model/highRES-AtLAST
65. Vásquez P, Devoto I, Ferrada P, et al (2021) Inspection Data Collection Tool for Field Testing of Photovoltaic Modules in the Atacama Desert. Energies 14:2409. https://doi.org/10.3390/en14092409
66. Viole I, Shen L, Ramirez Camargo L (2023a) Life Cycle Inventories (LCI) for Off-grid Hybrid Energy Systems using Photovoltaics, Batteries, and Hydrogen Storage. https://doi.org/10.5281/zenodo.8026737
67. Viole I, Valenzuela Venegas GA, Zeyringer M, Sartori S (2023b) A Renewable Power System for an Off-Grid Sustainable Telescope Fueled by Solar Power, Batteries and Green Hydrogen. SSRN Journal. https://doi.org/10.2139/ssrn.4376384
68. Viswanathan V, Mongird K, Franks R, et al (2022) 2022 Grid Energy Storage Technology Cost and Performance Assessment
69. Weber S, Peters JF, Baumann M, Weil M (2018) Life Cycle Assessment of a Vanadium Redox Flow Battery. Environ Sci Technol 52:10864–10873. https://doi.org/10.1021/acs.est.8b02073
70. World Bank (n.d.) CO2 emissions (metric tons per capita). In: World Bank Open Data. https://data.worldbank.org. Accessed 1 Jun 2023
71. Wulf C, Reuß M, Grube T, et al (2018) Life Cycle Assessment of hydrogen transport and distribution options. Journal of Cleaner Production 199:431–443. https://doi.org/10.1016/j.jclepro.2018.07.180
72. Yudhistira R, Khatiwada D, Sanchez F (2022) A comparative life cycle assessment of lithium-ion and lead-acid batteries for grid energy storage. Journal of Cleaner Production 358:131999. https://doi.org/10.1016/j.jclepro.2022.131999
73. Zhang S, Chen W (2022) Assessing the energy transition in China towards carbon neutrality with a probabilistic framework. Nat Commun 13:87. https://doi.org/10.1038/s41467-021-27671-0
74. Zhang Y, Zhang X, Lan L (2022) Robust optimization-based dynamic power generation mix evolution under the carbon-neutral target. Resources, Conservation and Recycling 178:106103. https://doi.org/10.1016/j.resconrec.2021.106103

Tables

Table 1
Selected impact categories and models

Impact Category	Unit	Impact Assessment Models
Climate change, total (CC)	kg CO_2e	Global warming potential (GWP100) (IPCC 2013)
Mineral resource depletion	kg Sb eq	Abiotic resource depletion (ADP ultimate reserves) (Guinée and Heijungs 1995; CML 2016)
Water use	m^3 water eq of deprived water	User deprivation potential (deprivation-weighted water consumption) (Boulay et al. 2018)

Table 2
Overview of compared scenarios, sizing optimized with highRES-AtLAST (Valenzuela Venegas 2022)

	Unit	Reference scenario	PD scenario	PDB scenario	PB scenario	PDBH scenario	PBH scenario
LCOE	\$/MWh	207.6	144.6	128.3	149.6	126.8	138.7
Initial installed capacity							
Diesel	MW	1.6	1.6	0.5		0.5	
PV	MW_p		2.4	4.5	6.3	4.9	6.5
AE	MW_e					1.2	1.7
CG	kg H_2					188.3	563.0
PEMFC	MW_e					0.2	0.4
LFP battery	MWh			16.8	25.3	12.4	16.7
Annual generation							
Diesel	MWh/year	7798.2	4594.9	511.9		461.2	0
PV			3203.4	7699.5	8254.7	9430.6	10891.4
PEMFC						1020.2	1603.6
LFP battery				3810.9	4210.2	2813.9	2601.2
Direct GHG emissions							
Total direct emissions over lifetime, 25 years	10^3 t CO_2e	167.8	98.8	11.0	0	9.9	0
Relative direct emissions	kg CO_2e/kWh	0.871	0.513	0.057	0	0.052	0

Table 3
Lifetime and needed replacement per 25 years of system components

System component	Part	Lifetime / degradation	Source	Replacements needed in 25 years
PV system	PV panel	1.56% degradation/yr	Average over median values of (Bouraiou et al. 2015; Vásquez et al. 2021; Hassan Daher et al. 2022; Bansal et al. 2022)	0.36 (based on 8% additional capacity every 5 years)
LFP batteries	Whole battery	2,640 cycles	(Viswanathan et al. 2022, p. 125)[1]	2.7
Electrolyzer	Stacks	60,000 hours	(Viswanathan et al. 2022, p. 126)	0.2
PEMFC	Stacks	40,000 hours	(Viswanathan et al. 2022, p. 126)	1.5

[1] This is Viswanathan et al. (2022)'s 2030 cycle life assumption for battery usage at 80% depth of discharge.

Table 4
Life cycle environmental impact associated with 7.7GWh/yr of power delivered to the telescope over a lifetime of 25 years

Impact category	Unit	Reference scenario	PD scenario	PDB scenario	PB scenario	PDBH scenario	PBH scenario
Life cycle GHG emissions (Climate change) - Total over 25 years and relative values	10^3 t CO_2e/lifetime	176.4	107.6	22.1	14.7	21.8	15.5
	kg CO_2e/kWh	0.917	0.559	0.115	0.077	0.113	0.080
Water use	10^6 m^3 water eq of deprived water/ lifetime	1.37	2.28	5.31	7.47	5.85	7.84
Mineral resource depletion	kg Sb (Antimony) eq/lifetime	90	264	1,115	1,610	1,002	1,338

Table 5
Sensitivity analysis of life cycle GHG emissions depending on different Chinese power mixes in 2030, associated with 7.7GWh/yr of power delivered to the telescope over a lifetime of 25 years

		Climate Change Impact in 10^3 t CO_2e / lifetime (relative change compared to reference transition power mix)				
Energy transition speed	**Carbon-neutral (RES and nuclear) generation share in Chinese power mix 2030**	**PD scenario**	**PDB scenario**	**PB scenario**	**PDBH scenario**	**PBH scenario**
Reference transition	54%	107.6	22.1	14.7	21.8	15.5
Faster transition	64.9%	107.5 (-0.1%)	21.8 (-1.3%)	14.3 (-2.8%)	21.5 (-1.3%)	15.1 (-2.4%)
Slower transition	35.5%	107.8 (+ 0.1%)	22.7 (+ 2.8%)	15.7 (+ 6.0%)	22.3 (+ 2.5%)	16.2 (+ 4.6%)

Figures

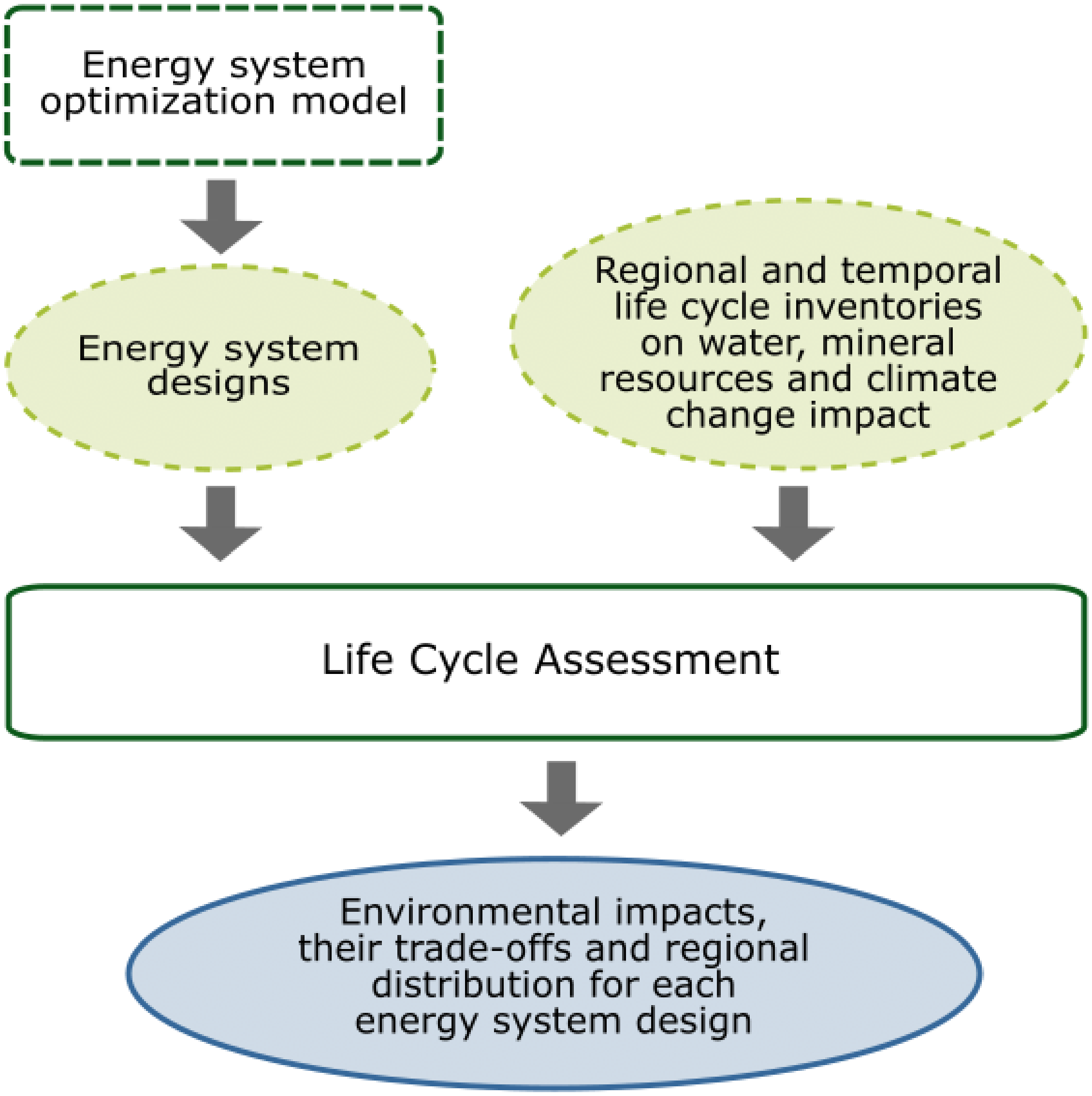

Figure 1

Flowchart of methodology, inputs to the *ex post* LCA developed in this study in green (energy system designs, regional and temporal inventories), outputs of the LCA in blue

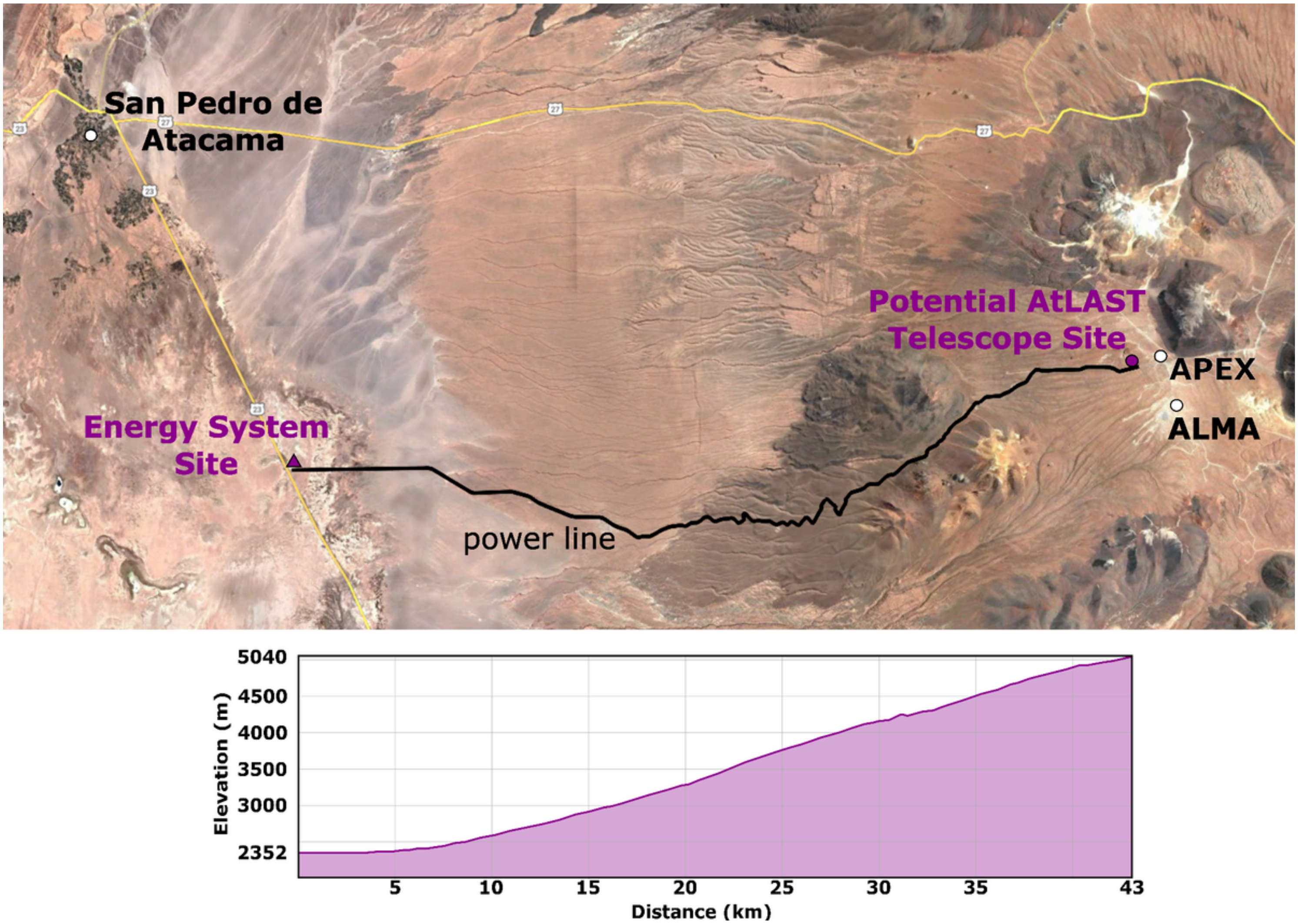

Figure 2

Map of the Chajnantor area with a potential site of AtLAST connected to the planned energy system site via a power line (in black), surrounded by the telescopes ALMA and APEX, and the city of San Pedro de Atacama; elevation between the two sites is shown in the bottom graph

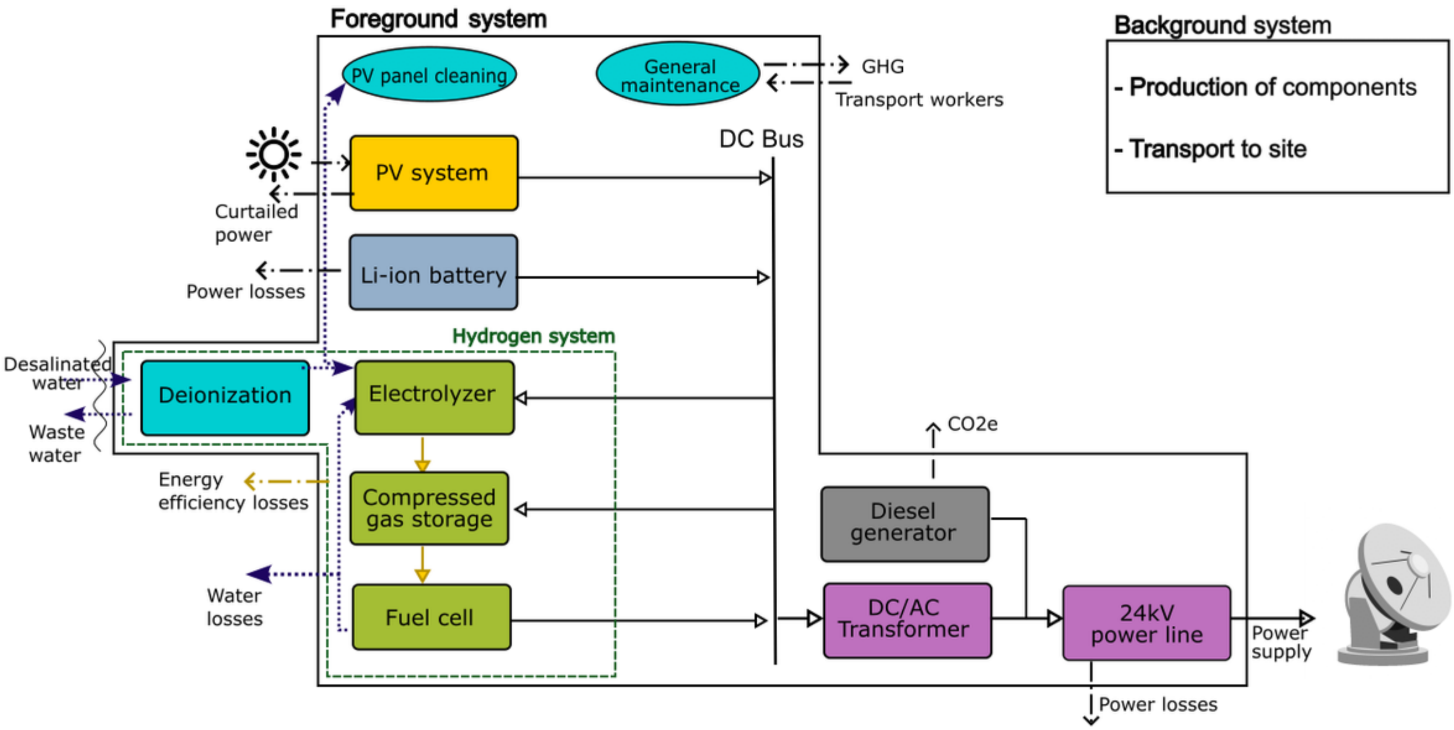

Figure 3

Flowchart of the system boundaries (black line), foreground system with energy system components

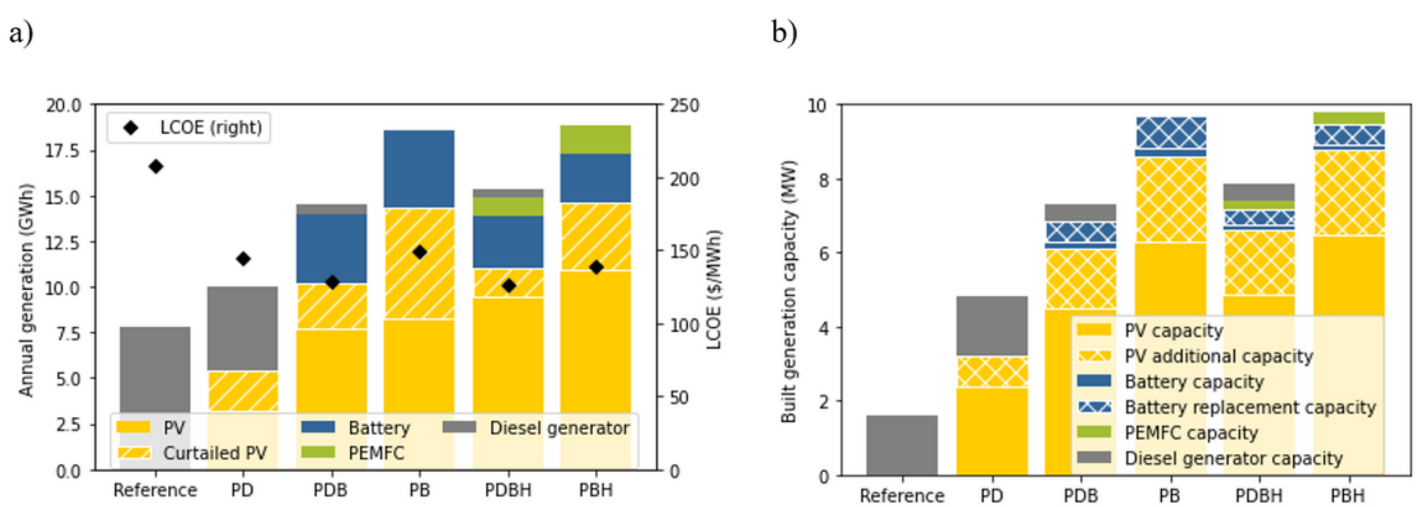

Figure 4

a) Annual generation (left axis), and levelized costs of electricity (LCOE, right axis); b) capacities installed of the six compared systems setups optimized with highRES-AtLAST to supply 7.7GWh$_e$/yr to the telescope

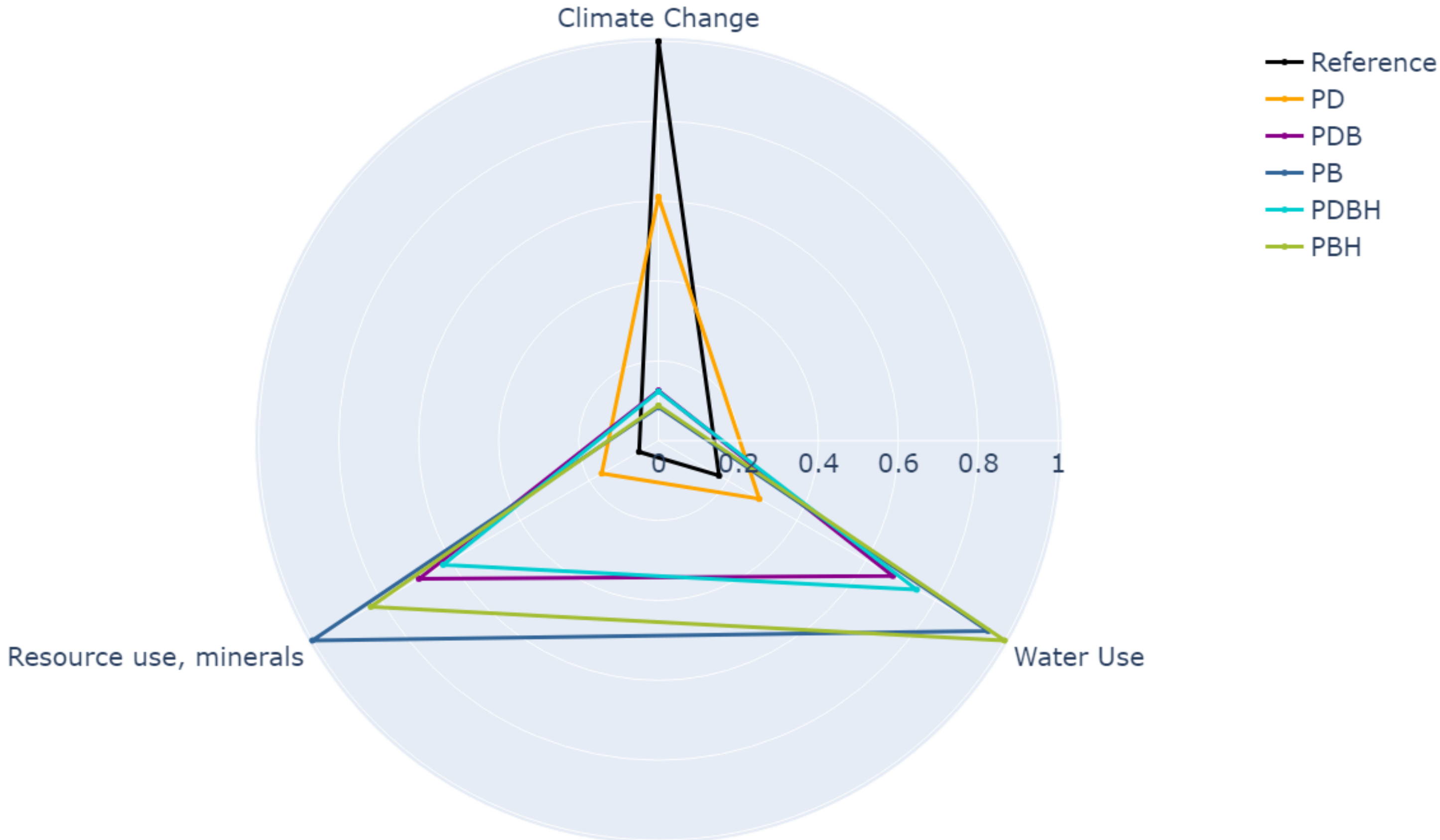

Figure 5

Relative environmental impacts of six compared energy system scenarios to supply 7.7GWh$_e$/yr to the telescope over a lifetime of 25 years, set in relation to maximum value within respective impact category

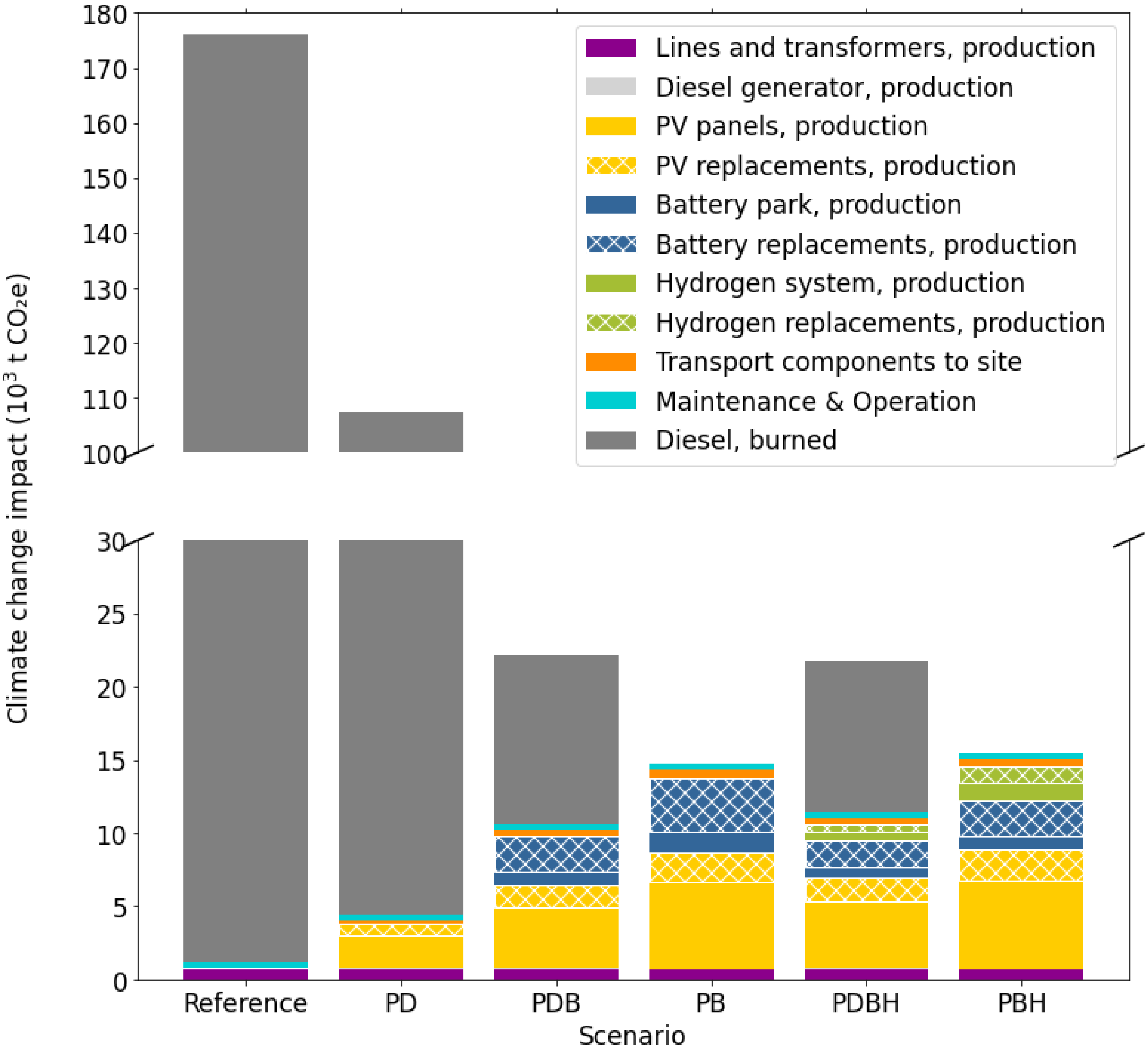

Figure 6

Climate change impact of the six energy system scenarios to supply $7.7 GWh_e$/yr to the telescope over a lifetime of 25 years, in 10^3 t CO_2e

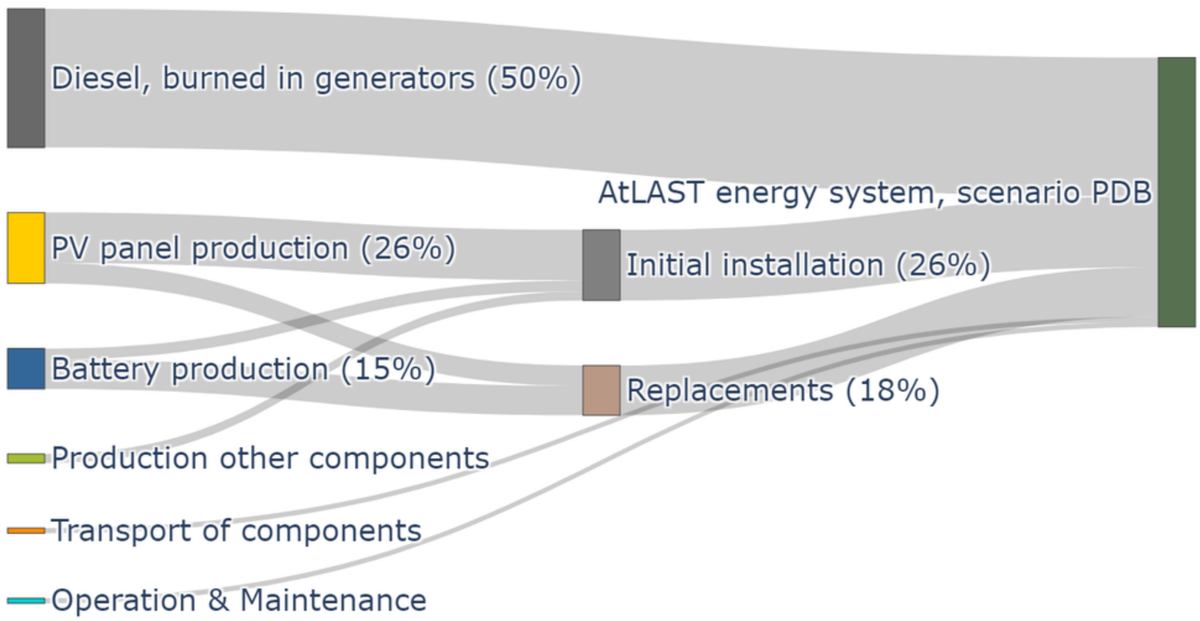

Figure 7

Relative contributions to the life cycle climate change impact on the PDB (PV, diesel and batteries) scenario to supply 7.7GWh$_e$/yr to the telescope over a lifetime of 25 years

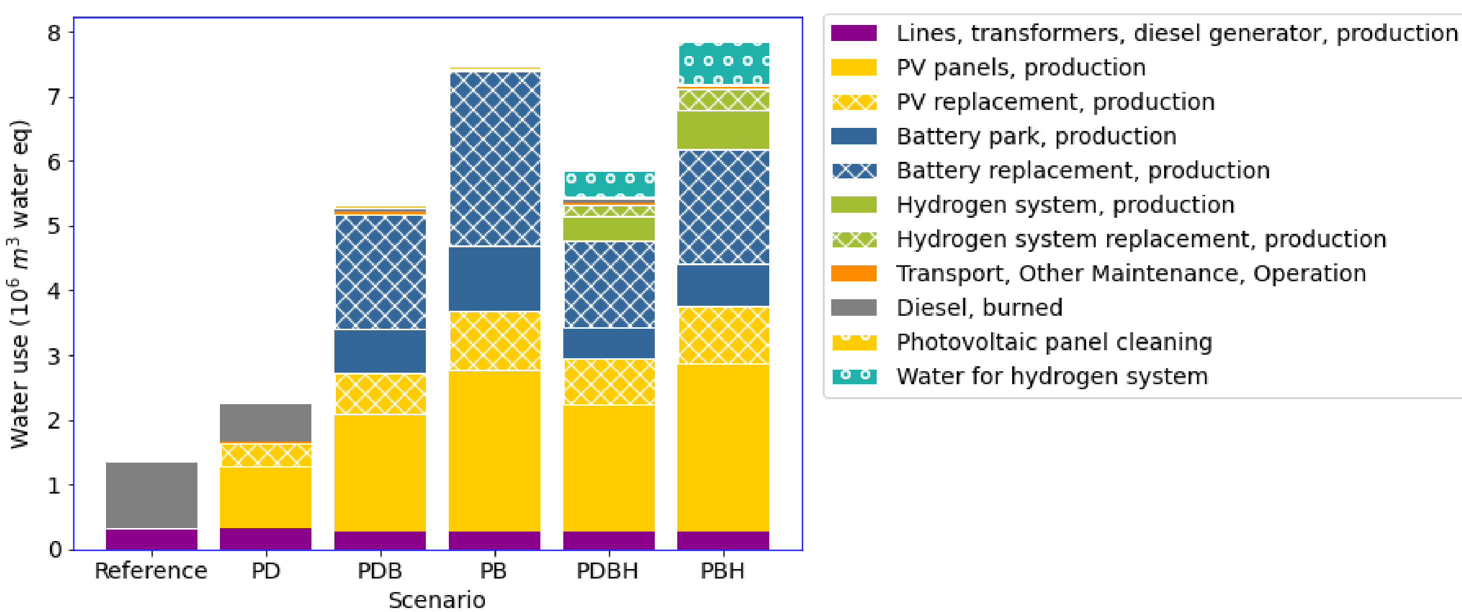

Figure 8

Water use of six energy system scenarios to supply 7.7GWh$_e$/yr to the telescope over a lifetime of 25 years, in 10^6 m^3 water eq

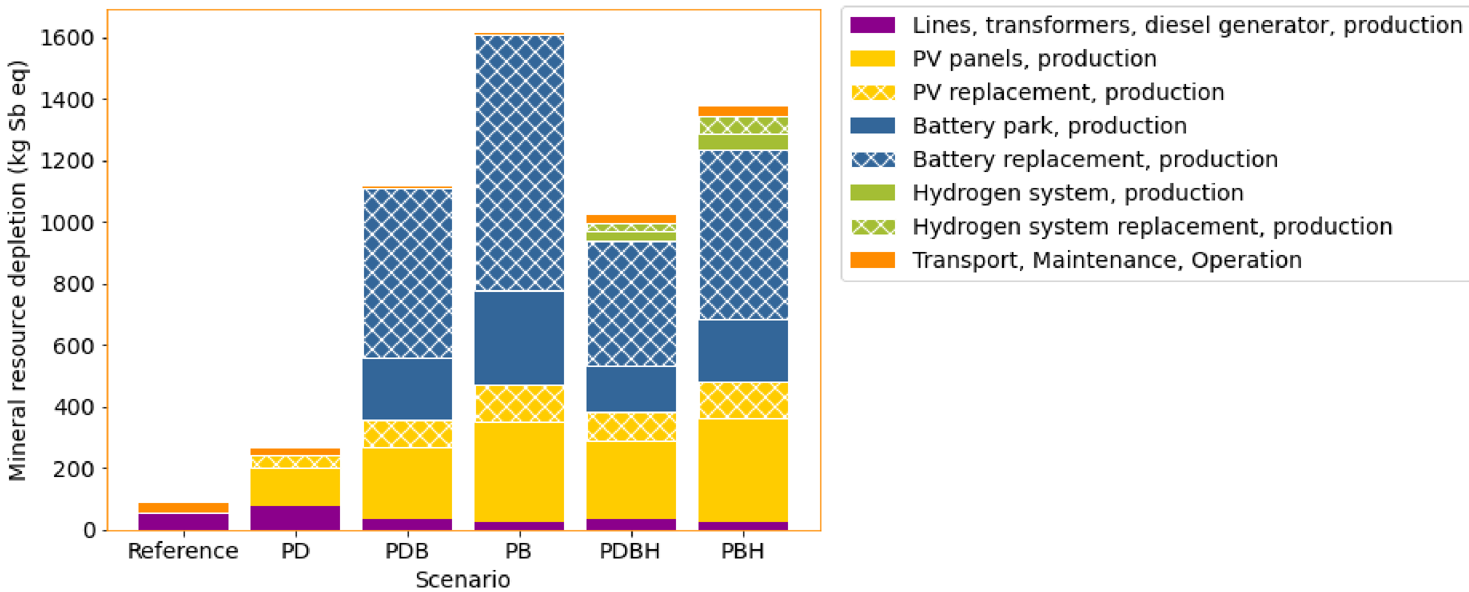

Figure 9

Mineral resource depletion of six energy system scenarios to supply 7.7GWh$_e$/yr to the telescope over a lifetime of 25 years, in kg Sb eq

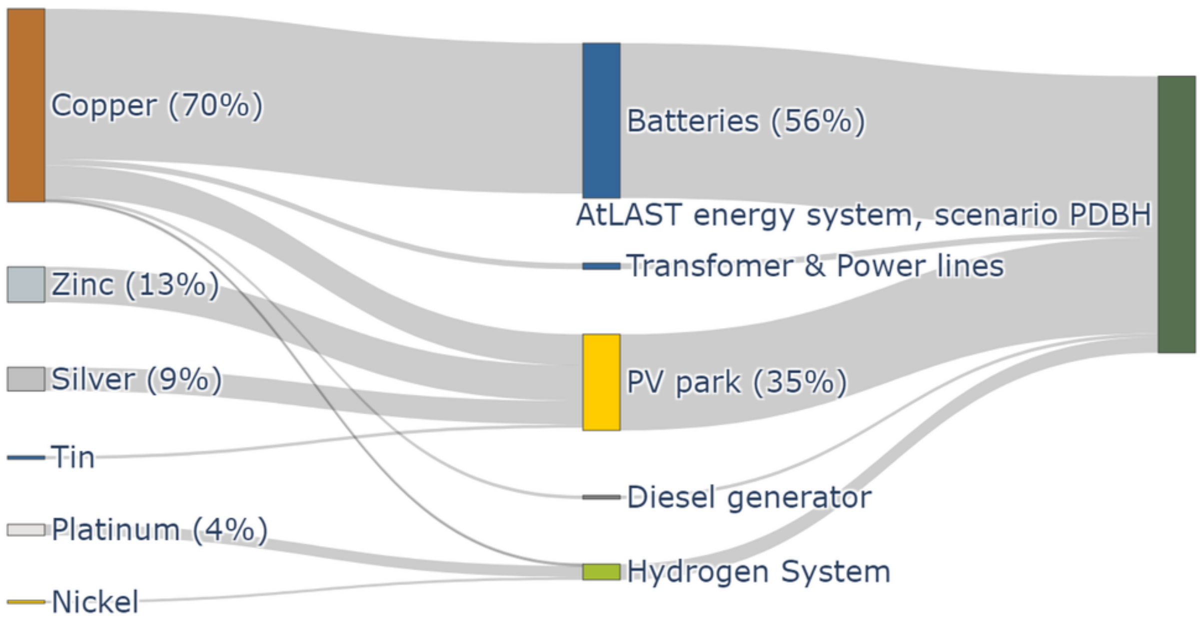

Figure 10

Relative contributions to the mineral resource depletion of the PDBH (PV, diesel, batteries, hydrogen system) scenario to supply 7.7GWh$_e$/yr to the telescope over a lifetime of 25 years

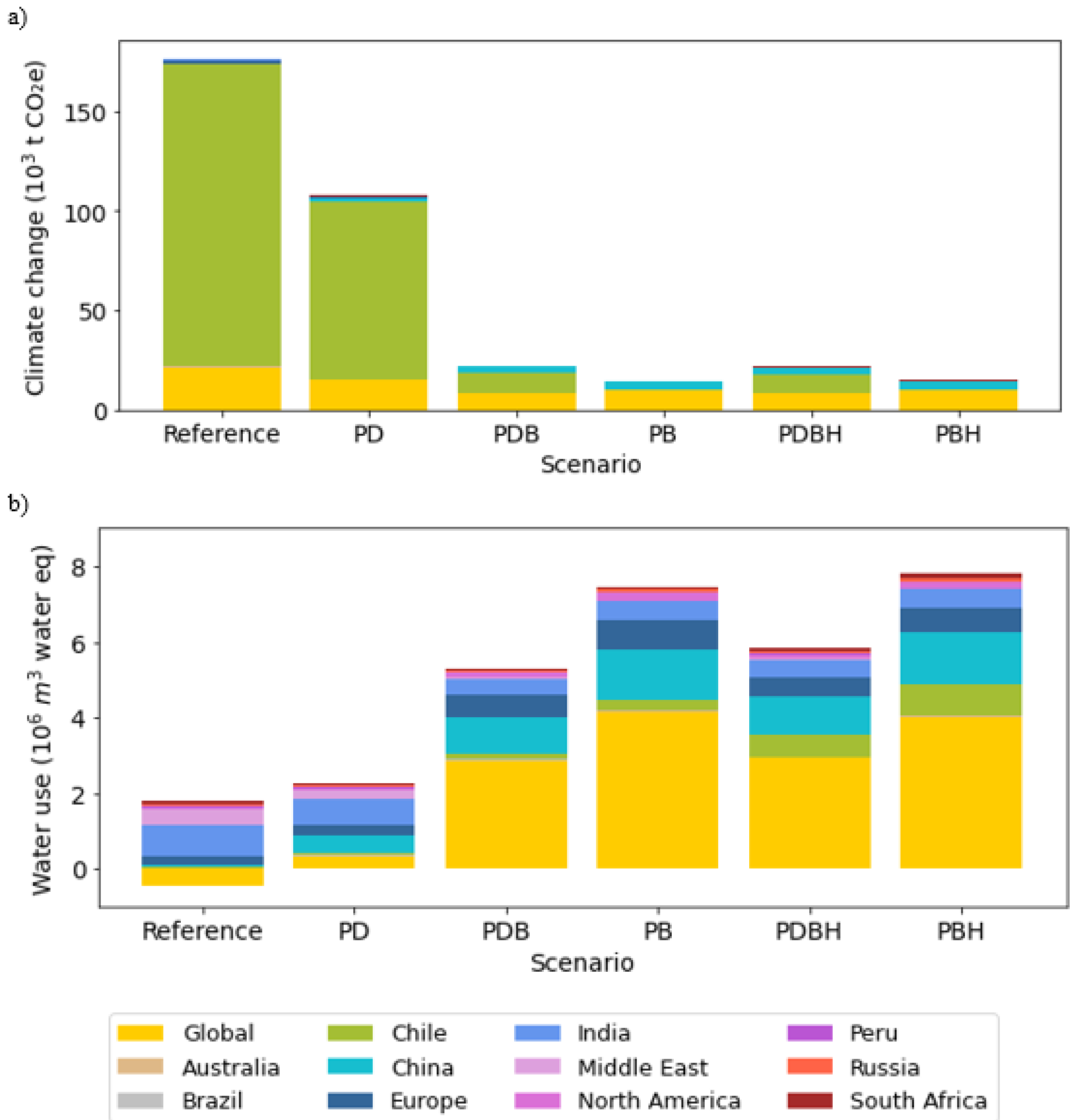

Figure 11

Global distribution of a) climate change, and b) water use of the six energy system scenarios to supply 7.7GWh$_e$/yr to the telescope over a lifetime of 25 years

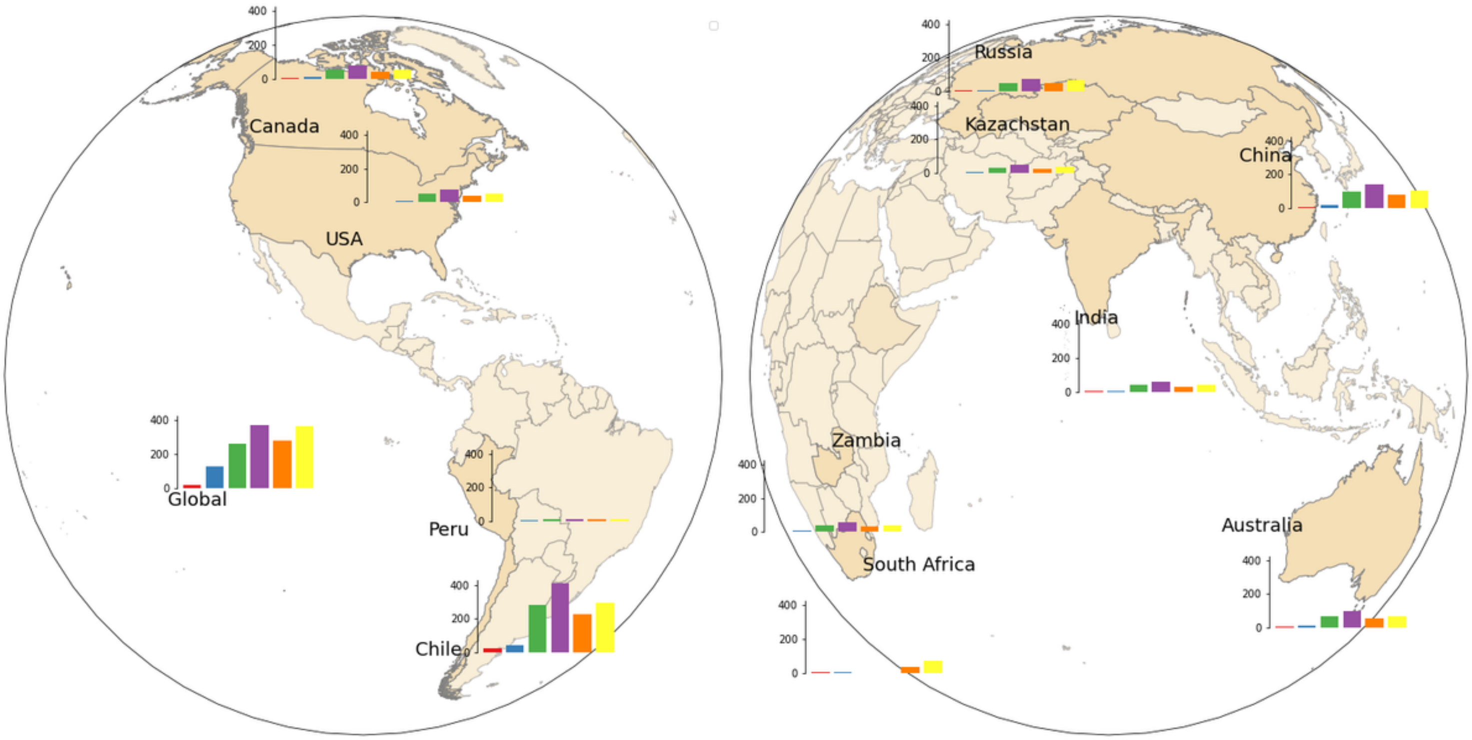

Figure 12

Map of global distribution of mineral resource depletion of the six energy system scenarios to supply 7.7GWh$_e$/yr to the telescope over a lifetime of 25 years, bars from left to right: Reference scenario, PD, PDB, PB, PDBH, PBH

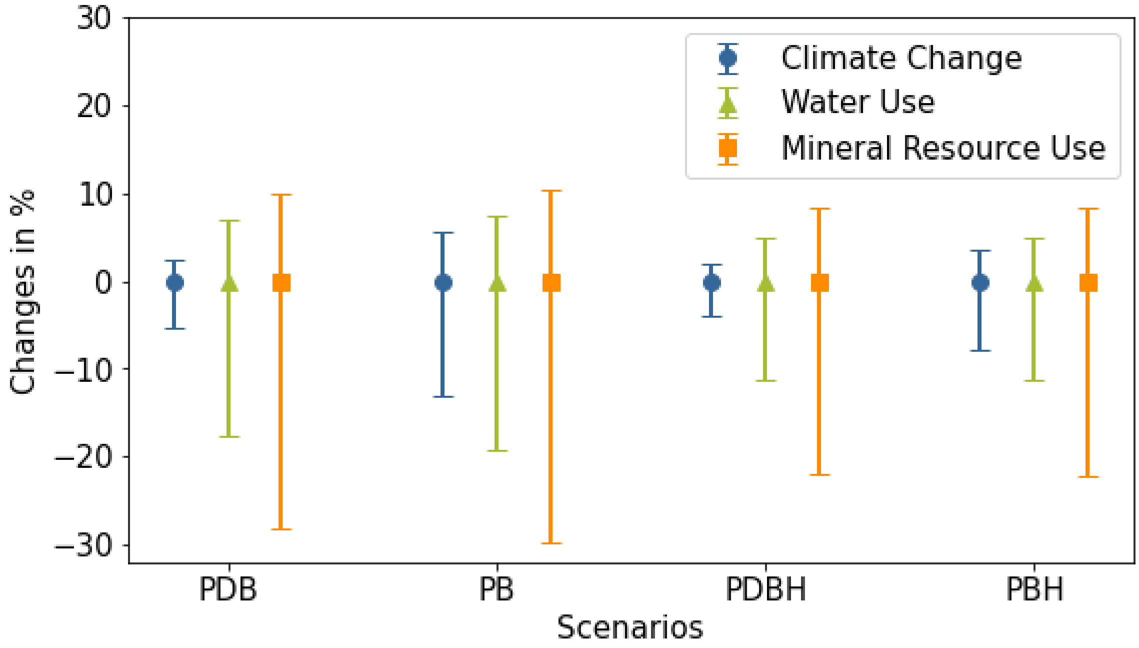

Figure 13

Sensitivity analysis of battery replacement rates, relative changes in climate change impact, water use, and mineral resource depletion with either 1.7 (lower boundary), 2.7 (baseline), and 3.3 replacements (upper boundary) of the batteries over the energy system's lifetime of 25 years

Supplementary Files

This is a list of supplementary files associated with this preprint. Click to download.

- Appendix.docx